On the rankability of visual embeddings

Ankit Sonthalia
University of Tübingen
ankit.sonthalia@uni-tuebingen.de

Arnas Uselis
University of Tübingen
arnas.uselis@uni-tuebingen.de

Seong Joon Oh
University of Tübingen

Abstract

We study whether visual embedding models capture continuous, ordinal attributes along linear directions, which we term *rank axes*. We define a model as *rankable* for an attribute if projecting embeddings onto such an axis preserves the attribute's order. Across 7 popular encoders and 9 datasets with attributes like age, crowd count, head pose, aesthetics, and recency, we find that many embeddings are inherently rankable. Surprisingly, a small number of samples, or even just two extreme examples, often suffice to recover meaningful rank axes, without full-scale supervision. These findings open up new use cases for image ranking in vector databases and motivate further study into the structure and learning of rankable embeddings. Our code is available at https://github.com/aktsonthalia/rankable-vision-embeddings.

1 Introduction

Visual embeddings are widely used for image retrieval. This relies on embeddings forming a metric space, where similar images are placed nearby. Modern visual encoders generally satisfy this property, and many systems depend on it in the form of vector databases.

Ranking is another core operation in databases. It allows users to navigate large collections by sorting, paginating, and filtering results. For instance, e-commerce platforms like Amazon benefit from ranking product images by visual quality or certain product-specific attributes (*e.g.,* ranking shoes by how formal they look).

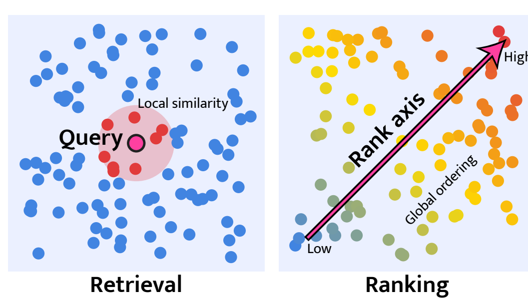

In this work, we ask: **are visual embeddings also rankable?** Retrieval relies on *local* similarity around a query. Ranking requires a *global* ordering along an attribute. Prior work has largely addressed the former. The global rankability of embeddings remains underexplored.

We define **rankability** as follows: given an embedding function f and a continuous attribute A (*e.g.,* "age"), we say f is rankable with respect to A if there exists a **rank axis** v_A such that the projection $v_A^\top f(x)$ preserves the correct order of the target attribute $A(x)$ over a dataset. For instance, if A denotes "age", this projection would sort face images from youngest to oldest.

We examine two questions: (1) Are visual embeddings rankable? (2) How easily can we recover the rank axis for a given attribute?

39th Conference on Neural Information Processing Systems (NeurIPS 2025).

To address (1), we evaluate 7 modern visual encoders, from ResNet to CLIP, across 9 datasets with 7 attributes: age, crowd count, 3 head pose angles (pitch, roll, yaw), image aesthetics, and recency. We find that many embedding spaces are indeed rankable (Section 3).

To address (2), we estimate the rank axis v_A with minimal supervision. The structure of the embedding space makes full-dataset regression unnecessary. In many cases, a handful of annotated samples and, in some cases, a pair of samples x_l (low) and x_h (high) already recover non-trivial ranking performance. For the latter case, we define the rank axis as $v_A = (f(x_h) - f(x_l))/\|f(x_h) - f(x_l)\|_2$. This opens up the possibility for fast ordering of new images by arbitrary attributes. For example, a photo app lets users sort selfies by age appearance. It uses CLIP embeddings and two reference images: one of a child and one of an elderly person. The app computes v_{age} without training. Users scroll from youngest-looking to oldest-looking faces in their album (Section 4).

Contributions:

1. We define and motivate rankability as a property of visual embeddings, distinct from retrieval.
2. We study rankability across modern encoders and real-valued attributes; results show that current embeddings are rankable.
3. We show that rank axes can sometimes be recovered using only two or a handful of labelled samples.

2 Related work

Embeddings for retrieval. Visual encoders are commonly used to index images in vector databases, enabling nearest neighbour search for retrieval tasks [42, 52, 33, 57]. This setup, known as deep metric learning [5, 6, 42], predates vision-language models like CLIP [52]. CLIP and related models shifted the focus to *cross-modal* similarity modelling, where vision and language share a joint embedding space used for classification [52], retrieval [75, 2], and captioning [39, 26]. While the majority of work in visual encoders is devoted to the understanding of the local similarity structure, we study how visual embeddings support *global* ranking instead of just local retrieval.

Improving embedding geometry and structure. Prior work has explored ways to improve the geometry of the embedding space. Order embeddings and hyperbolic representations have been used to model hierarchies [65, 21, 8, 51]. Training disentangled representation [71] is considered critical for compositionality, where attributes are assigned to certain linear subspaces [60, 3]. Others have defined concepts like uniformity and separability of the representations [70]. In this work, we focus on the analysis of a wide range of visual encoders, rather than introducing recipes for improvements.

Analysing embedding geometry and structure. A large body of work has examined the geometry and structure of CLIP's learned embedding space. CLIP and its derivatives have been studied extensively [4, 53, 32, 77]. Several works have reported modality gaps between vision and language embeddings [12]. Some studies point to the absence of certain structures and capabilities in CLIP representations: attribute-object bindings [31, 80, 25], or the association of attributes to corresponding instances. Others argue that much information is already present in CLIP representations, including parts-of-speech and linguistic structure [44], attribute-object bindings [24], and compositional attributes [62, 63]. The platonic representation hypothesis further suggests that models converge to similar internal structures [19]. In this work, we analyse the embedding geometry and structure for modern visual embeddings from the novel perspective of rankability.

Linearly probing an embedding. Linear probing is a fast and widely used method to test for the presence of concepts in visual embeddings [23, 18, 64]. It measures the accuracy of a linear classifier trained on intermediate-layer features, effectively testing whether a hyperplane can separate embeddings containing a concept from those that do not. This technique has been used to study the geometry of CLIP's embeddings [30] and to probe for specific information such as attribute-object bindings and compositionality [24, 62]. While effective for binary separability, linear probes are limited in capturing non-binary, ordinal, or relational structures [1]. Prior work has not directly analysed how *continuous* attributes are laid out in the embedding space. Our work extends this line of research by moving beyond concept detection to characterise the internal structure of embeddings along ordinal axes, introducing rankability as a new property not captured by prior probing methods.

Ordinal information in embeddings. Early works on relative and ordinal attributes explored how continuous visual attributes could be inferred and ranked [50, 36, 84, 14, 76]. However, these efforts were limited to smaller models and datasets. Recent studies have begun to examine ordinal signals in large pre-trained models. These include aligning CLIP with ordinal supervision [69], and applying CLIP or general VLMs to specific tasks such as aesthetics [74, 67], object counting [48, 20], crowd counting [35], and difference detection [56, 22]. Several works have adapted CLIP for ranking through prompt tuning [34], adapter-based methods [79] or regression-based fine-tuning [10, 68]. Despite these efforts, most focus on task-specific performance or modifying the embedding space, rather than understanding its internal ordinal structure in the embeddings themselves. Our work fills this gap by systematically analysing the rankable structure of existing visual encoders and revealing the presence of ordinal directions in their embedding spaces.

3 Are vision embeddings rankable?

We set out to answer the question. For this, we first formally define rankability and strategies to measure it (Section 3.1). We introduce the models and data used for our experiments in Section 3.2. We present results in Section 3.3.

Notation. Our experiments use RGB image datasets with real-valued attribute labels. We denote an image dataset as $X \subset \mathbb{R}^{3\times H\times W}$ and define an *ordinal attribute* A as a function $A : X \to Y \subset \mathbb{R}$ where Y is the range of possible labels and $A(x)$ is the ground-truth label for a given image x. An image encoder is a function $f : X \to \mathbb{R}^d$ where d is the dimensionality of the embedding space. We occasionally use the term "representation" to refer to an image encoder.

3.1 Rankability

We aim to characterize the *linear* structure of the ordinal information present in visual embedding spaces. Our definition of rankability then naturally emerges as follows.

Definition 1 (Rankability)**.** *A representation $f : X \to \mathbb{R}^d$ is **rankable** for an ordinal attribute A over an image dataset X if there exists a **rank axis** $v_A \in \mathcal{S}^{d-1}$, a $d-1$ dimensional unit sphere, such that for any $x_1, x_2 \in X$ with $A(x_1) \geq A(x_2)$, it follows that $v_A^\top f(x_1) \geq v_A^\top f(x_2)$.*

The above definition requires a rank axis v_A to exactly preserve the ordering provided by the attribute A over the dataset X. In practice, we measure rankability using the generalisation performance of the rank axis v_A learned on a training split X_{train} and tested on a disjoint split X_{test}. In this section, we obtain v_A via linear regression on the labelled samples: $\{(f(x_i), a_i)\}_i$, where $a_i \in \mathbb{R}$ is the ground-truth continuous attribute label for each x_i. In Section 4, we consider approaches that do not require access to the attribute labels a_i.

Spearman's rank correlation coefficient (SRCC), denoted as ρ serves as our primary metric quantifying the monotonicity of the relationship between the true ordinality of the attribute A and the predicted ranking along v_A. SRCC is widely used in related contexts [78].

We provide three reference points for the obtained rankability to contextualise the SRCC values:

(1) No-train ("lower bound"). Even for untrained visual encoders, the embeddings do not result in null rank correlation (ρ=0). In order to correctly capture the no-information baseline, we consider the performances of randomly initialized versions of each encoder considered [61]. The optimal rank axis v_A in this space serves as a lower bound for the rankability of the pretrained encoder.

(2) Nonlinear (upper bound for embedding). To estimate the total ordinal information in the given embedding, we use a two-layer multilayer perceptron (MLP), known to be a universal approximator [16]. Comparing against a non-linear regressor lets us estimate the proportion of ordinal information in an embedding that can be extracted linearly with a rank axis.

(3) Finetuning (upper bound for encoder architecture). To measure a broader upper bound indicating the capacity of the encoder architecture and the learnability of the attribute, we finetune the encoder. This conceptually envelops the nonlinear regression upper bound.

3.2 Experimental details

We provide further details on the list of attributes, datasets, encoder architectures, and the model selection protocol.

3.2.1 Attributes and datasets

In total, we use 9 datasets, covering 7 attributes. We provide a detailed breakdown in Table 1.

Table 1: **Datasets and attributes**. Summary of datasets used for evaluating the rankability of visual representations.

Attribute	Dataset	#Train-val	#Test	Label Range	Split
Age	UTKFace [83]	13,146	3,287	21–60	From [27]
	Adience [11]	∼14k	∼4k	8 age groups	Official 5-fold
Crowd count	UCF-QNRF [7]	1,201	334	49–12,865	Official
	ShanghaiTech-A [82]	300	182	33–3,139	Official
	ShanghaiTech-B [82]	400	316	9–578	Official
Pitch	BIWI Kinect [13]	10,493	4,531	$\pm 60°$	6 test seqs.
Yaw	BIWI Kinect	10,493	4,531	$\pm 75°$	6 test seqs.
Roll	BIWI Kinect	10,493	4,531	$\pm 45°$	6 test seqs.
Aesthetics	AVA [41]	230,686	4,692	Ratings (1–10)	From [78]
	KonIQ-10k [17]	8,058	2,015	Ratings (1–100)	Official
Image modernness	Historical Color Images [49]	1,060	265	5 decades	From [78]

3.2.2 Architectures

We test representative image-only and CLIP-based encoders. Among image-only encoders, we use the ResNet50 [15], ViT-B/32@224px [9], and ConvNeXtv2-L [73] architectures. Likewise, among CLIP encoders, we test the ResNet50, ViT-B/32, and ConvNeXt-L@320px variants. We also test DINOv2 [46] (ViT-B/14 variant). See Table 2 for more information.

Table 2: **Summary of vision encoders used in our study.** "Acronym" refers to how each model is denoted in our main results tables.

Acronym	Architecture	#Dims	Year	#Params	Type	Input Size
RN50	ResNet50	2048	2015	25.6M	ConvNet	224×224
ViTB32	ViT-B/32	768	2020	88.2M	Transformer	224×224
CNX	ConvNeXtV2	1536	2023	198M	ConvNet	224×224
DINO-B14	DINOv2 (ViT-B/14)	768	2023	86.6M	Transformer	518×518
CLIP-RN50	CLIP ResNet50	1024	2021	38.3M	ConvNet	224×224
CLIP-ViTB32	CLIP ViT-B/32	512	2021	87.8M	Transformer	224×224
CLIP-CNX	CLIP ConvNeXtV2	768	2023	199.8M	ConvNet	320×320

3.2.3 Hyperparameter tuning and model selection

Hyperparameters for reporting final performances on the test set are selected based on the best validation SRCC, using either official validation splits or holding them out from the corresponding training splits.

Linear and nonlinear regression. We test 30 random hyperparameter configurations per dataset-model pair. The initial learning rate is sampled from a log-uniform distribution over $[10^{-6},\ 10^{-1}]$ and decayed over a cosine schedule to zero, while the weight decay is sampled from a log-uniform distribution over $[10^{-7}, 10^{-4}]$. Data augmentation (horizontal flipping) is also toggled on or off randomly for a given run. We use 100 epochs and a batch size of 128 throughout. For nonlinear regression, we use a 2-layer MLP with 128 hidden dimensions and ReLU non-linearity.

Finetuning. For image-only ResNet50 and ConvNeXt encoders, we conduct a grid search over two encoder learning rates $(10^{-4}, 10^{-3})$ and two weight-decay rates $(0, 10^{-5})$. For ViT-B/32, DINOv2 and CLIP models, we conduct a larger grid search over three encoder learning rates $(10^{-7}, 10^{-6}, 10^{-5})$ and four weight-decay values $(0, 10^{-5}, 10^{-4}, 10^{-3})$. The downstream model always uses a learning rate of 0.1. We use 20 epochs for all runs. Batch size is fixed at 128, except for ConvNeXt-v2, DINOv2 and CLIP-ConvNeXt-v2, where batch size is reduced to 16 because of memory constraints. We use horizontal-flip augmentation in all finetuning runs to mitigate overfitting.

3.2.4 Compute resources

All experiments were conducted on a single NVIDIA A100 GPU with 40GB of memory. All primary experiments using frozen embeddings completed within 1–2 minutes, as we cache the embeddings. Finetuning experiments took between 1 and 24 hours each, depending on the dataset. In total, our experiments amounted to approximately 150 compute-days. We used the "stuned" Python library [55] for managing the experiments.

3.3 Results

Setup. The SRCC for the linear regressor measures the rankability of the underlying vision encoder, while the baselines (no-encoder, nonlinear regression and finetuning) provide reference points. We report our main results in Table 3 and Table 4. In Table 3, we average metrics across all architectures. Then in Table 4, we zoom into individual architectures while retaining only the rankability metric and averaging across all datasets that contain the same attribute. We also report qualitative results in Figure 1. Our observations vary across individual attributes and architectures, but some patterns emerge.

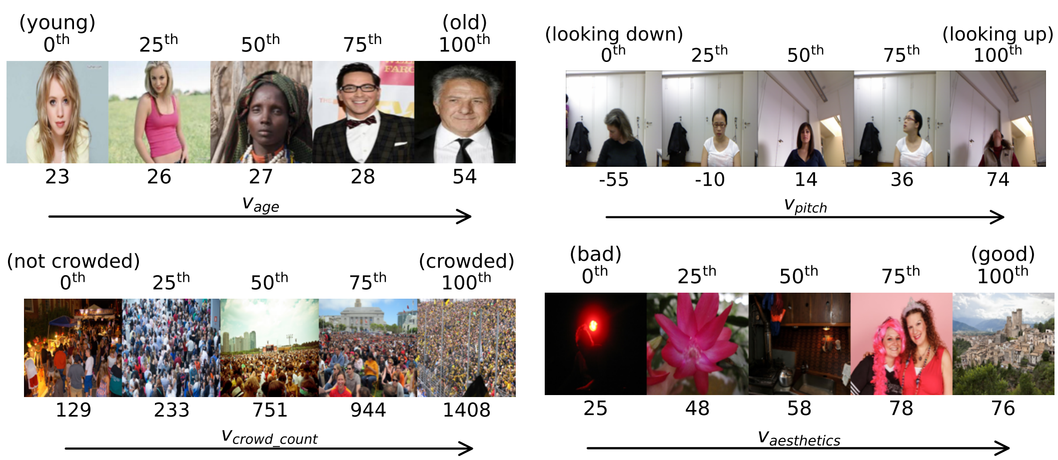

Figure 1: **Visualisation of rank axes.** We show r^{th} percentile samples along the rank axes found using linear regression over CLIP-ViT-B/32 embeddings from each respective dataset.

Average rankability of vision embeddings is non-trivially high. We observe in Table 3 that with respect to age on the Adience dataset, the average rankability of 0.861 is much higher than the no-train lower bound of 0.266, while the nonlinear and finetuned upper bounds (0.878 and 0.910) are only slightly higher in comparison. In fact, for all attributes except for yaw and roll, the average rankability is closer to the two upper bounds than to the lower bound.

Linear regression is often at par with dedicated SOTA efforts. Comparison with SOTA methods is outside of our main scope. We nevertheless find it interesting that often, linear regression over pretrained unmodified embeddings performs at par with dedicated SOTA efforts that require changing the underlying encoder or embeddings, or applying complex downstream models or specialised loss functions for the ranking task. For instance, as noted in Appendix E, on age estimation over UTKFace, linear regression achieves an MAE of 4.25, only slightly underperforming [78] (MAE = 3.83) and at par with [27] (MAE = 4.23). Our results suggest that the rankability of visual embeddings provides a

Table 3: **Vision embeddings are generally rankable**. Spearman rank correlation ρ between the true ranking of data samples and the predicted ranks. Higher is better. Results are averaged across all 7 architectures. **No-train**: Find v_A on the embeddings of a randomly-initialised encoder. **Rankability**: How well does v_A encode ordinal information? **Nonlinear**: Maximal non-linear ordinal information contained in embeddings. **Finetuned**: How learnable is the target attribute? For more information, see Section 3.1.

Attribute (Dataset)	**No-train** lower bound	**Rankability** main	**Nonlinear** upper bound	**Finetuned** upper bound
Age (UTKFace)	0.199	0.766	0.776	0.799
Age (Adience)	0.266	0.861	0.878	0.910
Crowd (UCF-QNRF)	0.220	0.843	0.854	0.886
Crowd Count (ST-A)	0.120	0.734	0.749	0.689
Crowd Count (ST-B)	0.135	0.869	0.887	0.840
Pitch (Kinect)	0.405	0.803	0.811	0.975
Yaw (Kinect)	0.078	0.434	0.597	0.967
Roll (Kinect)	0.151	0.218	0.326	0.859
Aesthetics (AVA)	0.156	0.653	0.692	0.693
Aesthetics (KonIQ-10k)	0.435	0.761	0.793	0.901
Recency (HCI)	0.324	0.680	0.688	0.722

Table 4: **Rankability across datasets and models**. Spearman's rank correlation ρ between the true ranking of data samples and the predicted ranks. Higher is better. See Table 2 for model details.

	Model						
Attribute (Dataset)	RN50	ViTB32	CNX	DINO-B14	CLIP-RN50	CLIP-ViTB32	CLIP-CNX
Age (UTKFace)	0.633	0.739	0.772	0.770	0.820	0.810	0.820
Age (Adience)	0.723	0.828	0.871	0.853	0.898	0.924	0.928
Crowd (UCF-QNRF)	0.864	0.837	0.810	0.788	0.870	0.870	0.860
Crowd (ST-A)	0.799	0.700	0.695	0.653	0.760	0.750	0.780
Crowd (ST-B)	0.879	0.878	0.867	0.821	0.890	0.860	0.890
Pitch (Kinect)	0.663	0.673	0.909	0.716	0.860	0.920	0.880
Yaw (Kinect)	0.624	0.305	0.384	0.804	0.120	0.360	0.440
Roll (Kinect)	0.352	0.196	0.298	0.512	0.090	0.020	0.060
Aesthetics (AVA)	0.589	0.609	0.644	0.566	0.700	0.710	0.750
Aesthetics (KonIQ-10k)	0.739	0.713	0.744	0.681	0.800	0.790	0.860
Recency (HCI)	0.600	0.592	0.631	0.571	0.780	0.770	0.820

strong, simple baseline that should be considered before applying such dedicated regression efforts. See Appendix E for detailed SOTA comparisons.

CLIP embeddings are more rankable than non-CLIP embeddings. We observe in Table 4 that on age, aesthetics, recency and pitch, the best CLIP encoder (*e.g.,* CLIP-ConvNeXt with an SRCC of 0.928 on Adience) wins out against the best non-CLIP encoder (*e.g.,* vanilla ConvNeXt with an SRCC of 0.871 on Adience). On crowd count, the best CLIP encoders are largely tied with the best non-CLIP encoders (*e.g.,* CLIP-RN50 at 0.870 vs vanilla RN50 at 0.864 for UCF-QNRF). On yaw and roll, DINO massively outperforms CLIP encoders (*e.g.,* 0.804 vs 0.440 for yaw). In conclusion, apart from isolated but interesting exceptions, CLIP encoders generally outperform or match non-CLIP encoders.

Some attributes are better ranked than others. For example, the average SRCC over the two age datasets is ~ 0.8 (see Table 3). Similar average SRCCs are observed for crowd count and pitch angle. Image aesthetics and recency are less well-ranked with average SRCCs between 0.65 and 0.75. Even within the same dataset (BIWI Kinect), yaw and roll angles with SRCCs of 0.434 and 0.218 are quite poorly ranked in comparison to pitch (0.803). We hypothesize that attribute-wise rankabilities are directly proportional to attribute-wise variety present in the training data. See also Appendix A.

Caveats. The current results are empirical, and our claims are based on the set of attributes considered in our study (we partially address this with a wider set of attributes in Appendix C). Despite following choices established in the literature, we may sometimes not uncover the most optimal finetuned upper bounds. A broader study involving theoretical support for rankability, using more ordinal attributes and possibly stronger upper bounds would be a promising direction for future work.

Takeaway from §3. In general, visual embeddings are highly rankable compared to both the lower bound and upper bound baselines, although there exist variations across attributes (*e.g.,* most encoders struggle to rank based on yaw and roll angles) and encoders (*e.g.,* CLIP embeddings are, in general, more rankable than non-CLIP embeddings).

4 How to (efficiently) find the rank axis?

In Section 3, we showed that visual embeddings are generally rankable. However, the rank axes v_A, determining the direction along which the continuous attribute A is sorted accordingly (Section 3.1), were learned using a lot of training data with continuous-attribute annotations that are typically expensive to collect. We examine whether rank axes can also be discovered in more sample- and label-efficient manners.

We organise the section by first tackling an easier setting with abundant data and then more challenging settings with less data available. We begin with the setting where we have a fraction of the dataset with continuous attribute labels (Section 4.1). Then, we examine the possibility to compute the rank axes with a few "extreme" points that require no cumbersome continuous attribute annotation (Section 4.2). For further practicality, we examine whether the obtained rank axes are resilient to domain shifts (Section 4.3). Finally, we discuss potential strategies to compute the rank axis in a zero-shot manner with text encoders in vision-language models (Section 4.4).

4.1 Learning using a fraction of the dataset with continuous attribute labels

In this section, we investigate the learnability of the rank axis v_A for an attribute of interest A, when fewer samples with continuous attribute annotations are available. We report the results in Figure 2. We choose the datasets UTKFace, Adience and AVA because of their relatively large sizes compared to the other datasets used in our experiments.

Only a fraction of training data is sufficient. For age on the Adience dataset, only $\sim$ 1k training samples out of over 11k are sufficient for covering as much as 95% of the gap between the SRCCs of the no-train baseline and full-dataset linear regression. Similarly, for image aesthetics on AVA (CLIP-ViT), only $\sim$ 16k (CLIP-ViT) or even $\sim$ 8k (CLIP-ConvNeXt) data points out of $\sim$ 230k are sufficient. It is evident that learning the rank axis often requires only a fraction of the original training dataset.

4.2 Learning using a small number of extreme pairs

We consider the practical scenario where a user wishes to sort their vector database using an arbitrary attribute A. They do not have access to continuous attribute annotations (as was assumed in Section 4.1), but can readily obtain a few samples at the "extremes" of the desired rank axis. We test the effectiveness of this approach.

Setup. Given training and test splits $\mathcal{X}_{\text{train}}$ and $\mathcal{X}_{\text{test}}$, respectively, we sample sets of images S_l and S_u from the lower and upper extremes of $\mathcal{X}_{\text{train}}$, respectively. This simulates the scenario where a user may obtain such "extreme" images using a readily available source like a Web search engine. Next, we

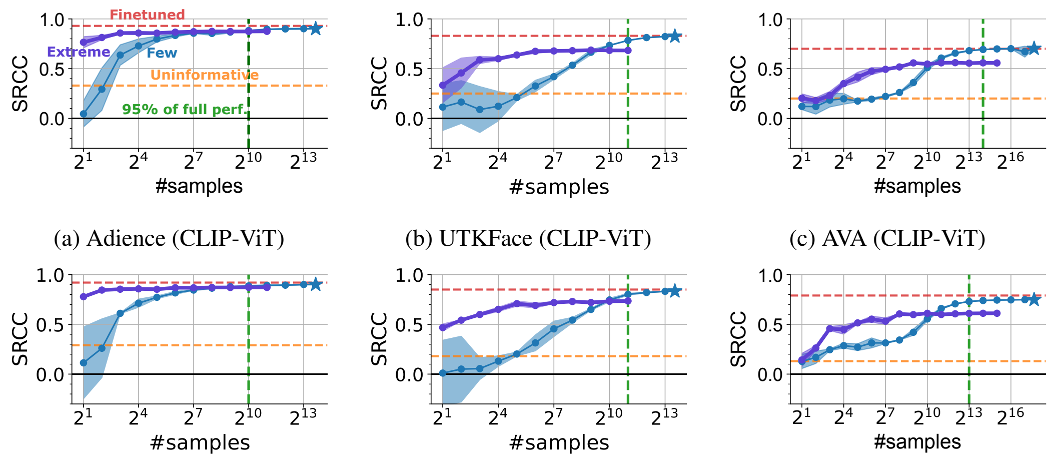

(a) Adience (CLIP-ViT) (b) UTKFace (CLIP-ViT) (c) AVA (CLIP-ViT)

(d) Adience (CLIP-ConvNeXt) (e) UTKFace (CLIP-ConvNeXt) (f) AVA (CLIP-ConvNeXt)

Figure 2: **Learning using a small number of samples with continuous labels vs extreme samples without continuous labels: extreme samples win out in the small-train-set regime.** **Extreme** refers to training using samples from the extreme ends of the ranking axis (without continuous labels), while **Few** refers to learning on continuously labelled samples. **Uninformative** refers to the no-train baseline while **Finetuned** refers to the finetuned upper bound. Dashed vertical lines labeled **95% of full perf.** indicate coverage of 95% of the gap between **Uninformative** and **Finetuned**. Full-dataset linear regression performance is denoted by a marker (★).

calculate the "lower extreme cluster" $x_l = \text{mean}(S_l)$ and "upper extreme cluster" $x_u = \text{mean}(S_u)$. Finally, the vector $v_A = \frac{x_u - x_l}{||x_u - x_l||}$ gives the rank axis (akin to a *steering vector* [54, 59]).

Observations. We report the results in Figure 2, comparing with the scenario where GT continuous attribute labels are available. We observe that when the size of the training dataset is extremely small (upto $\sim$ 1k), the extreme-pairs method performs better than or at par with regular training using an equal number of continuously labelled samples. This effect can be seen most prominently in the Adience dataset where a rank axis obtained from just two extreme samples achieves an SRCC of ~ 0.75 on average, while the vanilla training case results in an average SRCC close to 0. As the training dataset continues to grow in size, regular training with labelled data catches up and finally surpasses the extreme-pairs method. It is nevertheless striking that extreme pairs perform so well at lower sizes of the training dataset.

Takeaway. If one has an extremely small number of samples (1k or less), obtaining extreme samples from both ends of the rank axis (with no additional labeling) may constitute a better expenditure of resources than obtaining continuous attribute labels.

4.3 Robustness of rank axis

We now consider the case where there is no access to samples from the target distribution. Assuming that a rank axis was previously learned using some source distribution, how transferable is it to other distributions? We investigate this using three attributes: age, crowd count, and image aesthetics.

Setup. In our main experiments, we use two age datasets (UTKFace, Adience), three crowd count datasets (UCF-QNRF, ShanghaiTech-A, and ShanghaiTech-B), and two aesthetics datasets (AVA, KonIQ-10k). Within each set of datasets containing the same attribute, we then test how well a rank axis learned from one dataset transfers to another, and vice versa. We employ SRCC on the target dataset as our transferability metric in Table 5. Further, we also report cosine similarities between each pair of rank axes in Table 6. As reference points, we also report inter-attribute observations (*e.g.,* transfrability from an age dataset to an aesthetics dataset).

Transfer is non-trivial and asymmetric. For example, the rank axis learned from Adience has an SRCC of 0.680 on UTKFace, which is significantly higher than the SRCCs of the same rank axis on other datasets. Given that the two datasets have different labeling systems (especially with Adience labels being much more coarse than those in UTKFace), this is not immediately intuitive, or trivial,

Table 5: **Rank axis transferability**. Spearman rank correlation coefficients when a rank axis is *trained* on dataset i (rows) and *evaluated* on dataset j (columns).

		Evaluated on						
		Age (UTKFace)	Age (Adience)	Crowd (UCF-QNRF)	Crowd (ST-A)	Crowd (ST-B)	Aesthetics (AVA)	Aesthetics (KonIQ10k)
Trained on	Age (UTKFace)	+0.81	+0.55	−0.12	−0.11	−0.15	−0.07	+0.05
	Age (Adience)	+0.68	+0.91	−0.13	−0.10	−0.21	+0.01	−0.08
	Crowd (UCF-QNRF)	+0.16	−0.39	+0.87	+0.82	+0.66	+0.01	+0.07
	Crowd (ST-A)	+0.05	−0.14	+0.73	+0.75	+0.72	+0.13	+0.07
	Crowd (ST-B)	+0.31	+0.17	+0.41	+0.39	+0.86	+0.11	+0.05
	Aesthetics (AVA)	−0.12	−0.11	+0.22	+0.00	+0.49	+0.70	+0.45
	Aesthetics (KonIQ10k)	+0.06	−0.08	+0.03	+0.18	+0.05	+0.28	+0.79

and indicates the presence of some (albeit imperfect) "age" axis in the embedding space. At the same time, transfer in the opposite direction is not necessarily equally good (albeit still non-trivial), *i.e.,* a rank axis trained on UTKFace achieves an SRCC of only 0.55 on Adience.

Rank directions are non-trivially correlated. For example, the cosine similarity between age axes trained on UTKFace and Adience is 0.360. While this similarity is much lower than 1.0, it is still significant given the high dimensionality of the embedding space. This observation again indicates the presence of a "universal" age axis which was (albeit not perfectly) captured by regressors trained on both datasets. Notably, some unexpected correlations also emerge, *e.g.,* age (UTKFace) and aesthetics (KonIQ-10k) rank axes have a cosine similarity of 0.220. This suggests the presence of unintended correlations in the training / test data.

Table 6: **Cosine similarity of rank axes**. We compute geometric alignment of rank axes trained on dataset i (rows) and dataset j (columns).

		Dataset j						
		Age (UTKFace)	Age (Adience)	Crowd (UCF-QNRF)	Crowd (ST-A)	Crowd (ST-B)	Aesthetics (AVA)	Aesthetics (KonIQ10k)
Dataset i	Age (UTKFace)	+1.00	+0.36	+0.14	+0.08	+0.06	−0.04	+0.22
	Age (Adience)	+0.36	+1.00	+0.02	+0.04	+0.03	+0.03	+0.05
	Crowd (UCF-QNRF)	+0.14	+0.02	+1.00	+0.54	+0.26	+0.00	+0.21
	Crowd (ST-A)	+0.08	+0.04	+0.54	+1.00	+0.31	+0.01	+0.14
	Crowd (ST-B)	+0.06	+0.03	+0.26	+0.31	+1.00	+0.08	+0.07
	Aesthetics (AVA)	−0.04	+0.03	+0.00	+0.01	+0.08	+1.00	+0.29
	Aesthetics (KonIQ10k)	+0.22	+0.05	+0.21	+0.14	+0.07	+0.29	+1.00

4.4 Zero-shot setting

For VLMs, language is a potentially data-free approach to finding a rank axis. In principle, a text prompt could correspond to a rank axis in the embedding space. The SRCC of our linear regressors trained in Section 3 then sets an upper bound to the SRCC of any rank axis recovered via prompting. In this section, we investigate the gap between this linear regression upper bound and zero-shot prompt search.

Setup. We consider two zero-shot settings. In the **single-prompt** setting, the direction is defined by the embedding of a text prompt (*e.g.,* "a picture of an old person"). In the **text-difference** setting, the direction is defined by the difference between the embeddings of two text prompts, each describing one extreme of the given attribute (*e.g.,* "a picture of an empty room" and "a picture of a crowded room"). The latter setting is similar to the one used in [66]. We perform a prompt search over 500 prompts generated by GPT-4o [45] for the single-prompt setting, and 100 prompt pairs generated similarly for the text-difference setting. We report our results in Table 7.

Observations and takeaway. Overall, zero-shot methods are suboptimal. For instance, even the best zero-shot result corresponds to $\rho = 0.782$ on Adience vs. the corresponding linear model at $\rho = 0.917$. The gap is more pronounced for some attributes (*e.g.,* , $\rho = 0.449$ vs. $\rho = 0.790$ for image recency). While more optimal prompts may have been overlooked during the search, this also reflects a realistic setting where one exhausts all intuitive prompt choices. Currently, it is evident that language-based prompting lags considerably behind linear regression using image data, although the text-difference method improves upon vanilla prompting.

Table 7: **Zero-shot results.**

Attribute (Dataset)	**Zero-shot** One prompt	**Zero-shot** Difference	**Linear** upper bound
Age (UTKFace)	0.577	0.600	0.817
Age (Adience)	0.670	0.782	0.917
Crowd Count (UCF-QNRF)	0.523	0.315	0.867
Crowd Count (ST-A)	0.487	0.242	0.763
Crowd Count (ST-B)	0.590	0.535	0.880
Pitch (Kinect)	0.520	0.617	0.887
Yaw (Kinect)	0.117	0.060	0.307
Roll (Kinect)	-0.070	-0.010	0.057
Aesthetics (AVA)	0.367	0.410	0.720
Aesthetics (KonIQ-10k)	0.103	0.547	0.817
Recency (HCI)	0.190	0.449	0.790

Takeaway from §4. One may often efficiently discover the (almost) optimal rank axis using only a fraction of the total labelled data, or even pairs of extremes without continuous labels. Learned rank axes are quite transferable across different datasets, suggesting the presence of "universal" rank axes, although they may be somewhat spuriously entangled with the datasets used to obtain them.

5 Conclusion and future work

In this work, we investigate visual encoders for the presence of ordinal information. Extensive experiments reveal not only that such information is present, as indicated by the high Spearman rank correlation of nonlinear regressors, but also that most of the available ordinality is **linearly** encoded, as indicated by the small gap between the performances of linear and MLP regressors. The embedding space indeed possesses a "rankable" structure. This is unexpected and practically useful.

These findings provoke further questions. Most notably, the *linearity* of ordinal information suggests that one could potentially also characterise embeddings as interpretable collections of latent ordinal subspaces. This would involve discovering a far bigger set of ordinal attributes: we leave this exciting direction to future work.

Broader impact statement. Our work is largely a foundational analysis into the structure of embedding spaces and, as such, has no direct negative societal impacts. However, we highlight a few potential, indirect impacts. First, the ability to rank images containing personal or sensitive information (e.g. faces) with respect to arbitrary attributes may risk exposing certain individuals that are at the extreme ends of a spectrum (e.g. income level). Second, ordering individuals along a single attribute axis, such as gender, may reinforce existing stereotypes and offend and marginalize certain demographic groups.

Acknowledgements. This work was supported by the German Federal Ministry of Education and Research (BMBF): Tübingen AI Center, FKZ: 01IS18039A. The authors thank the International Max Planck Research School for Intelligent Systems (IMPRS-IS) for supporting Ankit Sonthalia and Arnas Uselis. The authors are also grateful to Wei-Hsiang Yu, the first author of [78], for helpful insights.

References

[1] Guillaume Alain and Yoshua Bengio. "Understanding intermediate layers using linear classifier probes". In: *arXiv preprint arXiv:1610.01644* (2016).

[2] Alberto Baldrati et al. "Conditioned and composed image retrieval combining and partially fine-tuning CLIP-based features". In: *2022 IEEE/CVF Conference on Computer Vision and Pattern Recognition Workshops (CVPRW)* (2022), pp. 4955–4964. URL: https://api.semanticscholar.org/CorpusId:251034454.

[3] Davide Berasi et al. "Not Only Text: Exploring Compositionality of Visual Representations in Vision-Language Models". In: *ArXiv* abs/2503.17142 (2025). URL: https://api.semanticscholar.org/CorpusId:277244112.

[4] Ting Chen et al. "A Simple Framework for Contrastive Learning of Visual Representations". In: *Proceedings of the 37th International Conference on Machine Learning*. International Conference on Machine Learning. PMLR, Nov. 21, 2020, pp. 1597–1607. URL: https://proceedings.mlr.press/v119/chen20j.html.

[5] Wei Chen et al. "Deep Learning for Instance Retrieval: A Survey". In: *IEEE Transactions on Pattern Analysis and Machine Intelligence* 45 (2021), pp. 7270–7292. URL: https://api.semanticscholar.org/CorpusId:245837930.

[6] Wei Chen et al. "Deep learning for instance retrieval: A survey". In: *IEEE Transactions on Pattern Analysis and Machine Intelligence* 45.6 (2022), pp. 7270–7292.

[7] "Composition Loss for Counting, Density Map Estimation and Localization in Dense Crowds". In: Haroon Idrees et al. *Lecture Notes in Computer Science*. Cham: Springer International Publishing, 2018, pp. 544–559. ISBN: 978-3-030-01215-1 978-3-030-01216-8. DOI: 10.1007/978-3-030-01216-8_33. URL: https://link.springer.com/10.1007/978-3-030-01216-8_33.

[8] Karan Desai et al. "Hyperbolic Image-Text Representations". In: *ArXiv* abs/2304.09172 (2023). URL: https://arxiv.org/pdf/2304.09172.pdf.

[9] Alexey Dosovitskiy et al. *An Image is Worth 16x16 Words: Transformers for Image Recognition at Scale*. arXiv:2010.11929. June 2021. DOI: 10.48550/arXiv.2010.11929. URL: http://arxiv.org/abs/2010.11929.

[10] Yao Du et al. *Teach CLIP to Develop a Number Sense for Ordinal Regression*. Aug. 7, 2024. DOI: 10.48550/arXiv.2408.03574. arXiv: 2408.03574 [cs]. URL: http://arxiv.org/abs/2408.03574. Pre-published.

[11] Eran Eidinger, Roee Enbar, and Tal Hassner. "Age and Gender Estimation of Unfiltered Faces". In: *IEEE Transactions on Information Forensics and Security* 9.12 (Dec. 2014), pp. 2170–2179. ISSN: 1556-6021. DOI: 10.1109/TIFS.2014.2359646. URL: https://ieeexplore.ieee.org/document/6906255.

[12] Abrar Fahim, Alex Murphy, and Alona Fyshe. "Its Not a Modality Gap: Characterizing and Addressing the Contrastive Gap". In: *ArXiv* abs/2405.18570 (2024). URL: https://api.semanticscholar.org/CorpusId:270095104.

[13] Gabriele Fanelli et al. "Real Time Head Pose Estimation from Consumer Depth Cameras". In: *Pattern Recognition*. Ed. by Rudolf Mester and Michael Felsberg. Red. by David Hutchison et al. Vol. 6835. Berlin, Heidelberg: Springer Berlin Heidelberg, 2011, pp. 101–110. ISBN: 978-3-642-23122-3 978-3-642-23123-0. DOI: 10.1007/978-3-642-23123-0_11. URL: http://link.springer.com/10.1007/978-3-642-23123-0_11.

[14] Hu Han et al. "Heterogeneous face attribute estimation: A deep multi-task learning approach". In: *IEEE transactions on pattern analysis and machine intelligence* 40.11 (2017), pp. 2597–2609.

[15] Kaiming He et al. "Deep Residual Learning for Image Recognition". In: *2016 IEEE Conference on Computer Vision and Pattern Recognition (CVPR)*. 2016 IEEE Conference on Computer Vision and Pattern Recognition (CVPR). Las Vegas, NV, USA: IEEE, June 2016, pp. 770–778. ISBN: 978-1-4673-8851-1. DOI: 10.1109/CVPR.2016.90. URL: http://ieeexplore.ieee.org/document/7780459/.

[16] Kurt Hornik, Maxwell Stinchcombe, and Halbert White. "Multilayer feedforward networks are universal approximators". In: *Neural networks* 2.5 (1989), pp. 359–366.

[17] Vlad Hosu et al. "KonIQ-10k: An Ecologically Valid Database for Deep Learning of Blind Image Quality Assessment". In: *IEEE Transactions on Image Processing* 29 (2020), pp. 4041–4056. ISSN: 1057-7149, 1941-0042. DOI: 10.1109/TIP.2020.2967829. arXiv: 1910.06180 [cs]. URL: http://arxiv.org/abs/1910.06180.

[18] Yunshi Huang et al. "Lp++: A surprisingly strong linear probe for few-shot clip". In: *Proceedings of the IEEE/CVF Conference on Computer Vision and Pattern Recognition*. 2024, pp. 23773–23782.

[19] Minyoung Huh et al. "The platonic representation hypothesis". In: *arXiv preprint arXiv:2405.07987* (2024).

[20] Ruixiang Jiang, Lingbo Liu, and Changwen Chen. "CLIP-Count: Towards Text-Guided Zero-Shot Object Counting". In: *Proceedings of the 31st ACM International Conference on Multimedia*. Oct. 26, 2023, pp. 4535–4545. DOI: `10.1145/3581783.3611789`. arXiv: `2305.07304 [cs]`. URL: `http://arxiv.org/abs/2305.07304`.

[21] Valentin Khrulkov et al. "Hyperbolic Image Embeddings". In: *2020 IEEE/CVF Conference on Computer Vision and Pattern Recognition (CVPR)* (2019), pp. 6417–6427. URL: `http://ieeexplore.ieee.org/stamp/stamp.jsp?tp=%5C&arnumber=9156432`.

[22] Jihyung Kil et al. *CompBench: A Comparative Reasoning Benchmark for Multimodal LLMs*. July 23, 2024. DOI: `10.48550/arXiv.2407.16837`. arXiv: `2407.16837 [cs]`. URL: `http://arxiv.org/abs/2407.16837`. Pre-published.

[23] Been Kim et al. "Interpretability beyond feature attribution: Quantitative testing with concept activation vectors (tcav)". In: *International conference on machine learning*. PMLR. 2018, pp. 2668–2677.

[24] Darina Koishigarina, Arnas Uselis, and Seong Joon Oh. *CLIP Behaves like a Bag-of-Words Model Cross-modally but Not Uni-modally*. Feb. 8, 2025. DOI: `10.48550/arXiv.2502.03566`. arXiv: `2502.03566 [cs]`. URL: `http://arxiv.org/abs/2502.03566`. Pre-published.

[25] Darina Koishigarina, Arnas Uselis, and Seong Joon Oh. "CLIP Behaves like a Bag-of-Words Model Cross-modally but not Uni-modally". In: *arXiv preprint arXiv:2502.03566* (2025).

[26] Chia-Wen Kuo and Z. Kira. "Beyond a Pre-Trained Object Detector: Cross-Modal Textual and Visual Context for Image Captioning". In: *2022 IEEE/CVF Conference on Computer Vision and Pattern Recognition (CVPR)* (2022), pp. 17948–17958. URL: `https://api.semanticscholar.org/CorpusId:248572429`.

[27] Maksim Kuprashevich and Irina Tolstykh. *MiVOLO: Multi-input Transformer for Age and Gender Estimation*. Sept. 22, 2023. DOI: `10.48550/arXiv.2307.04616`. arXiv: `2307.04616 [cs]`. URL: `http://arxiv.org/abs/2307.04616`. Pre-published.

[28] Alina Kuznetsova et al. "The Open Images Dataset V4: Unified image classification, object detection, and visual relationship detection at scale". In: *International Journal of Computer Vision* 128.7 (July 2020). arXiv:1811.00982 [cs], pp. 1956–1981. ISSN: 0920-5691, 1573-1405. DOI: `10.1007/s11263-020-01316-z`. URL: `http://arxiv.org/abs/1811.00982`.

[29] Seon-Ho Lee, Nyeong-Ho Shin, and Chang-Su Kim. "Geometric Order Learning for Rank Estimation". In: (2022).

[30] Meir Yossef Levi and Guy Gilboa. *The Double-Ellipsoid Geometry of CLIP*. Nov. 21, 2024. DOI: `10.48550/arXiv.2411.14517`. arXiv: `2411.14517 [cs]`. URL: `http://arxiv.org/abs/2411.14517`. Pre-published.

[31] Martha Lewis et al. "Does clip bind concepts? probing compositionality in large image models". In: *arXiv preprint arXiv:2212.10537* (2022).

[32] Junnan Li et al. "Align before fuse: Vision and language representation learning with momentum distillation". In: *Advances in Neural Information Processing Systems*. Vol. 34. 2021, pp. 9694–9705.

[33] Junnan Li et al. "BLIP: Bootstrapping Language-Image Pre-training for Unified Vision-Language Understanding and Generation". In: *Proceedings of the 39th International Conference on Machine Learning*. International Conference on Machine Learning. PMLR, June 28, 2022, pp. 12888–12900. URL: `https://proceedings.mlr.press/v162/li22n.html`.

[34] Wanhua Li et al. *OrdinalCLIP: Learning Rank Prompts for Language-Guided Ordinal Regression*. Oct. 1, 2022. DOI: `10.48550/arXiv.2206.02338`. arXiv: `2206.02338 [cs]`. URL: `http://arxiv.org/abs/2206.02338`. Pre-published.

[35] Dingkang Liang et al. *CrowdCLIP: Unsupervised Crowd Counting via Vision-Language Model*. Apr. 9, 2023. DOI: `10.48550/arXiv.2304.04231`. arXiv: `2304.04231 [cs]`. URL: `http://arxiv.org/abs/2304.04231`. Pre-published.

[36] Lucy Liang and Kristen Grauman. "Beyond comparing image pairs: Setwise active learning for relative attributes". In: *Proceedings of the IEEE conference on Computer Vision and Pattern Recognition*. 2014, pp. 208–215.

[37] Yiming Ma, Victor Sanchez, and Tanaya Guha. *CLIP-EBC: CLIP Can Count Accurately through Enhanced Blockwise Classification*. Version 3. Mar. 25, 2025. DOI: 10.48550/arXiv.2403.09281. arXiv: 2403.09281 [cs]. URL: http://arxiv.org/abs/2403.09281. Pre-published.

[38] Loic Matthey et al. *dSprites: Disentanglement testing Sprites dataset*. https://github.com/deepmind/dsprites-dataset/. 2017.

[39] Ron Mokady, Amir Hertz, and Amit H Bermano. "Clipcap: Clip prefix for image captioning". In: *arXiv preprint arXiv:2111.09734* (2021).

[40] Stylianos Moschoglou et al. "AgeDB: The First Manually Collected, In-the-Wild Age Database". en. In: *2017 IEEE Conference on Computer Vision and Pattern Recognition Workshops (CVPRW)*. Honolulu, HI, USA: IEEE, July 2017, pp. 1997–2005. ISBN: 978-1-5386-0733-6. DOI: 10.1109/CVPRW.2017.250. URL: http://ieeexplore.ieee.org/document/8014984/.

[41] N. Murray, L. Marchesotti, and F. Perronnin. "AVA: A Large-Scale Database for Aesthetic Visual Analysis". In: *2012 IEEE Conference on Computer Vision and Pattern Recognition*. 2012 IEEE Conference on Computer Vision and Pattern Recognition (CVPR). Providence, RI: IEEE, June 2012. DOI: 10.1109/cvpr.2012.6247954. URL: http://ieeexplore.ieee.org/document/6247954/.

[42] Kevin Musgrave, Serge Belongie, and Ser-Nam Lim. "A metric learning reality check". In: *Computer Vision–ECCV 2020: 16th European Conference, Glasgow, UK, August 23–28, 2020, Proceedings, Part XXV 16*. Springer. 2020, pp. 681–699.

[43] Kartik Narayan et al. *FaceXFormer: A Unified Transformer for Facial Analysis*. arXiv:2403.12960 [cs]. Mar. 2025. DOI: 10.48550/arXiv.2403.12960. URL: http://arxiv.org/abs/2403.12960.

[44] James Oldfield et al. "Parts of Speech-Grounded Subspaces in Vision-Language Models". In: *ArXiv* abs/2305.14053 (2023). URL: https://api.semanticscholar.org/CorpusId:258841517.

[45] OpenAI et al. *GPT-4o System Card*. Oct. 25, 2024. DOI: 10.48550/arXiv.2410.21276. arXiv: 2410.21276 [cs]. URL: http://arxiv.org/abs/2410.21276. Pre-published.

[46] Maxime Oquab et al. *DINOv2: Learning Robust Visual Features without Supervision*. en. arXiv:2304.07193 [cs]. Feb. 2024. URL: http://arxiv.org/abs/2304.07193.

[47] Maxime Oquab et al. *DINOv2: Learning Robust Visual Features without Supervision*. Feb. 2, 2024. DOI: 10.48550/arXiv.2304.07193. arXiv: 2304.07193 [cs]. URL: http://arxiv.org/abs/2304.07193. Pre-published.

[48] Roni Paiss et al. *Teaching CLIP to Count to Ten*. Feb. 23, 2023. DOI: 10.48550/arXiv.2302.12066. arXiv: 2302.12066 [cs]. URL: http://arxiv.org/abs/2302.12066. Pre-published.

[49] Frank Palermo, James Hays, and Alexei A. Efros. "Dating Historical Color Images". In: *Computer Vision – ECCV 2012*. Ed. by Andrew Fitzgibbon et al. Red. by David Hutchison et al. Vol. 7577. Berlin, Heidelberg: Springer Berlin Heidelberg, 2012, pp. 499–512. ISBN: 978-3-642-33782-6 978-3-642-33783-3. DOI: 10.1007/978-3-642-33783-3_36. URL: http://link.springer.com/10.1007/978-3-642-33783-3_36.

[50] Devi Parikh and Kristen Grauman. "Relative Attributes". In: *2011 International Conference on Computer Vision*. 2011 IEEE International Conference on Computer Vision (ICCV). Barcelona, Spain: IEEE, Nov. 2011, pp. 503–510. ISBN: 978-1-4577-1102-2 978-1-4577-1101-5 978-1-4577-1100-8. DOI: 10.1109/ICCV.2011.6126281. URL: http://ieeexplore.ieee.org/document/6126281/.

[51] Zhi Qiao et al. "HYDEN: Hyperbolic Density Representations for Medical Images and Reports". In: *International Conference on Computational Linguistics*. 2024. URL: https://api.semanticscholar.org/CorpusId:271903357.

[52] Alec Radford et al. "Learning Transferable Visual Models From Natural Language Supervision". In: *International Conference on Machine Learning*. 2021. URL: https://arxiv.org/pdf/2103.00020.pdf.

[53] Alec Radford et al. "Learning Transferable Visual Models From Natural Language Supervision". In: *Proceedings of the 38th International Conference on Machine Learning*. International Conference on Machine Learning. PMLR, July 1, 2021, pp. 8748–8763. URL: `https://proceedings.mlr.press/v139/radford21a.html`.

[54] Nina Rimsky et al. "Steering Llama 2 via Contrastive Activation Addition". In: *Proceedings of the 62nd Annual Meeting of the Association for Computational Linguistics (Volume 1: Long Papers)*. ACL 2024. Ed. by Lun-Wei Ku, Andre Martins, and Vivek Srikumar. Bangkok, Thailand: Association for Computational Linguistics, Aug. 2024, pp. 15504–15522. DOI: `10.18653/v1/2024.acl-long.828`. URL: `https://aclanthology.org/2024.acl-long.828/`.

[55] Alexander Rubinstein and Arnas Uselis. *STAI-tuned Experiment Scheduler: Structured Experiment Management with Google Sheets, Weights & Biases, and HPC Integration*. `https://github.com/arubique/stnd`. GitHub repository. Utility code for reproducible and streamlined experiment management with Google Sheets integration, W&B logging, and HPC support (e.g., Slurm). 2025.

[56] Dylan Sam et al. *Finetuning CLIP to Reason about Pairwise Differences*. Sept. 15, 2024. DOI: `10.48550/arXiv.2409.09721`. arXiv: `2409.09721 [cs]`. URL: `http://arxiv.org/abs/2409.09721`. Pre-published.

[57] Konstantin Schall et al. "Improving Image Encoders for General-Purpose Nearest Neighbor Search and Classification". In: *Proceedings of the 2023 ACM International Conference on Multimedia Retrieval*. ICMR '23. Thessaloniki, Greece: Association for Computing Machinery, 2023, pp. 57–66. ISBN: 9798400701788. DOI: `10.1145/3591106.3592266`. URL: `https://doi.org/10.1145/3591106.3592266`.

[58] Christoph Schuhmann et al. *LAION-400M: Open Dataset of CLIP-Filtered 400 Million Image-Text Pairs*. arXiv:2111.02114 [cs]. Nov. 2021. DOI: `10.48550/arXiv.2111.02114`. URL: `http://arxiv.org/abs/2111.02114`.

[59] Curt Tigges et al. *Linear Representations of Sentiment in Large Language Models*. Oct. 23, 2023. DOI: `10.48550/arXiv.2310.15154`. arXiv: `2310.15154 [cs]`. URL: `http://arxiv.org/abs/2310.15154`. Pre-published.

[60] Matthew Trager et al. "Linear Spaces of Meanings: Compositional Structures in Vision-Language Models". In: *2023 IEEE/CVF International Conference on Computer Vision (ICCV)* (2023), pp. 15349–15358. URL: `https://api.semanticscholar.org/CorpusId:257766294`.

[61] Dmitry Ulyanov, Andrea Vedaldi, and Victor Lempitsky. "Deep image prior". In: *Proceedings of the IEEE conference on computer vision and pattern recognition*. 2018, pp. 9446–9454.

[62] Arnas Uselis, Andrea Dittadi, and Seong Joon Oh. "BEYOND DECODABILITY: LINEAR FEATURE SPACES ENABLE VISUAL COMPOSITIONAL GENERALIZATION". In: Workshop on Spurious Correlation and Shortcut Learning: Foundations and Solutions. Mar. 6, 2025.

[63] Arnas Uselis, Andrea Dittadi, and Seong Joon Oh. "Does Data Scaling Lead to Visual Compositional Generalization?" In: *arXiv preprint arXiv:2507.07102* (2025).

[64] Arnas Uselis and Seong Joon Oh. "Intermediate Layer Classifiers for OOD Generalization". In: *International Conference on Learning Representations (ICLR)*. 2025.

[65] Ivan Vendrov et al. "Order-Embeddings of Images and Language". In: *CoRR* abs/1511.06361 (2015). URL: `https://arxiv.org/pdf/1511.06361.pdf`.

[66] Jianyi Wang, Kelvin C. K. Chan, and Chen Change Loy. *Exploring CLIP for Assessing the Look and Feel of Images*. Nov. 23, 2022. DOI: `10.48550/arXiv.2207.12396`. arXiv: `2207.12396 [cs]`. URL: `http://arxiv.org/abs/2207.12396`. Pre-published.

[67] Jianyi Wang, Kelvin C.K. Chan, and Chen Change Loy. "Exploring CLIP for Assessing the Look and Feel of Images". In: *Proceedings of the Thirty-Seventh AAAI Conference on Artificial Intelligence and Thirty-Fifth Conference on Innovative Applications of Artificial Intelligence and Thirteenth Symposium on Educational Advances in Artificial Intelligence*. Vol. 37. AAAI'23/IAAI'23/EAAI'23. AAAI Press, Feb. 7, 2023, pp. 2555–2563. ISBN: 978-1-57735-880-0. DOI: `10.1609/aaai.v37i2.25353`. URL: `https://doi.org/10.1609/aaai.v37i2.25353`.

[68] Rui Wang et al. "Learning-to-Rank Meets Language: Boosting Language-Driven Ordering Alignment for Ordinal Classification". In: (2023).

[69] Rui Wang et al. "Learning-to-rank meets language: Boosting language-driven ordering alignment for ordinal classification". In: *Advances in Neural Information Processing Systems* 36 (2023).

[70] Tongzhou Wang and Phillip Isola. "Understanding Contrastive Representation Learning through Alignment and Uniformity on the Hypersphere". In: *ArXiv* abs/2005.10242 (2020). URL: https://arxiv.org/pdf/2005.10242.pdf.

[71] Xin Wang et al. "Disentangled representation learning". In: *IEEE Transactions on Pattern Analysis and Machine Intelligence* (2024).

[72] Ross Wightman. *PyTorch Image Models*. https://github.com/rwightman/pytorch-image-models. 2019. DOI: 10.5281/zenodo.4414861.

[73] Sanghyun Woo et al. *ConvNeXt V2: Co-designing and Scaling ConvNets with Masked Autoencoders*. Jan. 2, 2023. DOI: 10.48550/arXiv.2301.00808. arXiv: 2301.00808 [cs]. URL: http://arxiv.org/abs/2301.00808. Pre-published.

[74] Liwu Xu et al. "Clip brings better features to visual aesthetics learners". In: *arXiv preprint arXiv:2307.15640* (2023).

[75] Lewei Yao et al. "Filip: Fine-grained interactive language-image pre-training". In: *arXiv preprint arXiv:2111.07783* (2021).

[76] Aron Yu and Kristen Grauman. "Just noticeable differences in visual attributes". In: *Proceedings of the IEEE International Conference on Computer Vision*. 2015, pp. 2416–2424.

[77] Jiahui Yu et al. "CoCa: Contrastive Captioners are Image-Text Foundation Models". In: *Transactions on Machine Learning Research* (2022). URL: https://openreview.net/forum?id=M_Vb2v063oH.

[78] Wei-Hsiang Yu et al. "RANKING-AWARE ADAPTER FOR TEXT-DRIVEN IMAGE ORDERING WITH CLIP". In: *ICLR* (2025).

[79] Wei-Hsiang Yu et al. *Ranking-Aware Adapter for Text-Driven Image Ordering with CLIP*. Dec. 9, 2024. DOI: 10.48550/arXiv.2412.06760. arXiv: 2412.06760 [cs]. URL: http://arxiv.org/abs/2412.06760. Pre-published.

[80] Mert Yuksekgonul et al. "When and why vision-language models behave like bags-of-words, and what to do about it?" In: *arXiv preprint arXiv:2210.01936* (2022).

[81] Kaiwen Zha et al. "Rank-N-Contrast: Learning Continuous Representations for Regression". In: *NeurIPS* (2023).

[82] Yingying Zhang et al. "Single-Image Crowd Counting via Multi-Column Convolutional Neural Network". In: *2016 IEEE Conference on Computer Vision and Pattern Recognition (CVPR)*. 2016 IEEE Conference on Computer Vision and Pattern Recognition (CVPR). Las Vegas, NV, USA: IEEE, June 2016, pp. 589–597. ISBN: 978-1-4673-8851-1. DOI: 10.1109/CVPR.2016.70. URL: http://ieeexplore.ieee.org/document/7780439/.

[83] Zhifei Zhang, Yang Song, and Hairong Qi. *Age Progression/Regression by Conditional Adversarial Autoencoder*. Mar. 28, 2017. DOI: 10.48550/arXiv.1702.08423. arXiv: 1702.08423 [cs]. URL: http://arxiv.org/abs/1702.08423. Pre-published.

[84] Daniel Zoran et al. "Learning Ordinal Relationships for Mid-Level Vision". In: *Proceedings of the IEEE International Conference on Computer Vision (ICCV)*. Dec. 2015.

NeurIPS Paper Checklist

The checklist is designed to encourage best practices for responsible machine learning research, addressing issues of reproducibility, transparency, research ethics, and societal impact. Do not remove the checklist: **The papers not including the checklist will be desk rejected.** The checklist should follow the references and follow the (optional) supplemental material. The checklist does NOT count towards the page limit.

Please read the checklist guidelines carefully for information on how to answer these questions. For each question in the checklist:

- You should answer [Yes] , [No] , or [NA] .
- [NA] means either that the question is Not Applicable for that particular paper or the relevant information is Not Available.
- Please provide a short (1–2 sentence) justification right after your answer (even for NA).

The checklist answers are an integral part of your paper submission. They are visible to the reviewers, area chairs, senior area chairs, and ethics reviewers. You will be asked to also include it (after eventual revisions) with the final version of your paper, and its final version will be published with the paper.

The reviewers of your paper will be asked to use the checklist as one of the factors in their evaluation. While "[Yes] " is generally preferable to "[No] ", it is perfectly acceptable to answer "[No] " provided a proper justification is given (e.g., "error bars are not reported because it would be too computationally expensive" or "we were unable to find the license for the dataset we used"). In general, answering "[No] " or "[NA] " is not grounds for rejection. While the questions are phrased in a binary way, we acknowledge that the true answer is often more nuanced, so please just use your best judgment and write a justification to elaborate. All supporting evidence can appear either in the main paper or the supplemental material, provided in appendix. If you answer [Yes] to a question, in the justification please point to the section(s) where related material for the question can be found.

IMPORTANT, please:

- **Delete this instruction block, but keep the section heading "NeurIPS Paper Checklist"**,
- **Keep the checklist subsection headings, questions/answers and guidelines below.**
- **Do not modify the questions and only use the provided macros for your answers**.

1. **Claims**

   Question: Do the main claims made in the abstract and introduction accurately reflect the paper's contributions and scope?

   Answer: [Yes]

   Justification: Our main claim is that modern visual encoders have "rankable" embedding spaces and that rankings can often be recovered using just a fraction of the original dataset. We provide empirical justification for the first part of the claim through extensive empirical validation in Section 3, and for the second part in Section 4.

   Guidelines:

   - The answer NA means that the abstract and introduction do not include the claims made in the paper.
   - The abstract and/or introduction should clearly state the claims made, including the contributions made in the paper and important assumptions and limitations. A No or NA answer to this question will not be perceived well by the reviewers.
   - The claims made should match theoretical and experimental results, and reflect how much the results can be expected to generalize to other settings.
   - It is fine to include aspirational goals as motivation as long as it is clear that these goals are not attained by the paper.

2. **Limitations**

   Question: Does the paper discuss the limitations of the work performed by the authors?

Answer: [Yes]

Justification: We discuss the caveats of our approach wherever they apply: in particular, we discuss them at the end of Section 3.

Guidelines:

- The answer NA means that the paper has no limitation while the answer No means that the paper has limitations, but those are not discussed in the paper.
- The authors are encouraged to create a separate "Limitations" section in their paper.
- The paper should point out any strong assumptions and how robust the results are to violations of these assumptions (e.g., independence assumptions, noiseless settings, model well-specification, asymptotic approximations only holding locally). The authors should reflect on how these assumptions might be violated in practice and what the implications would be.
- The authors should reflect on the scope of the claims made, e.g., if the approach was only tested on a few datasets or with a few runs. In general, empirical results often depend on implicit assumptions, which should be articulated.
- The authors should reflect on the factors that influence the performance of the approach. For example, a facial recognition algorithm may perform poorly when image resolution is low or images are taken in low lighting. Or a speech-to-text system might not be used reliably to provide closed captions for online lectures because it fails to handle technical jargon.
- The authors should discuss the computational efficiency of the proposed algorithms and how they scale with dataset size.
- If applicable, the authors should discuss possible limitations of their approach to address problems of privacy and fairness.
- While the authors might fear that complete honesty about limitations might be used by reviewers as grounds for rejection, a worse outcome might be that reviewers discover limitations that aren't acknowledged in the paper. The authors should use their best judgment and recognize that individual actions in favor of transparency play an important role in developing norms that preserve the integrity of the community. Reviewers will be specifically instructed to not penalize honesty concerning limitations.

3. **Theory assumptions and proofs**

   Question: For each theoretical result, does the paper provide the full set of assumptions and a complete (and correct) proof?

   Answer: [NA]

   Justification: Our paper is purely empirical and we do not include any theoretical results.

   Guidelines:

   - The answer NA means that the paper does not include theoretical results.
   - All the theorems, formulas, and proofs in the paper should be numbered and cross-referenced.
   - All assumptions should be clearly stated or referenced in the statement of any theorems.
   - The proofs can either appear in the main paper or the supplemental material, but if they appear in the supplemental material, the authors are encouraged to provide a short proof sketch to provide intuition.
   - Inversely, any informal proof provided in the core of the paper should be complemented by formal proofs provided in appendix or supplemental material.
   - Theorems and Lemmas that the proof relies upon should be properly referenced.

4. **Experimental result reproducibility**

   Question: Does the paper fully disclose all the information needed to reproduce the main experimental results of the paper to the extent that it affects the main claims and/or conclusions of the paper (regardless of whether the code and data are provided or not)?

   Answer: [Yes]

Justification: Section 3.2 details the model architectures and datasets used by us (all of which are freely available online), as well as our hyperparameter searches. Using these details, it is straightforward to reproduce our conclusions.

Guidelines:

- The answer NA means that the paper does not include experiments.
- If the paper includes experiments, a No answer to this question will not be perceived well by the reviewers: Making the paper reproducible is important, regardless of whether the code and data are provided or not.
- If the contribution is a dataset and/or model, the authors should describe the steps taken to make their results reproducible or verifiable.
- Depending on the contribution, reproducibility can be accomplished in various ways. For example, if the contribution is a novel architecture, describing the architecture fully might suffice, or if the contribution is a specific model and empirical evaluation, it may be necessary to either make it possible for others to replicate the model with the same dataset, or provide access to the model. In general. releasing code and data is often one good way to accomplish this, but reproducibility can also be provided via detailed instructions for how to replicate the results, access to a hosted model (e.g., in the case of a large language model), releasing of a model checkpoint, or other means that are appropriate to the research performed.
- While NeurIPS does not require releasing code, the conference does require all submissions to provide some reasonable avenue for reproducibility, which may depend on the nature of the contribution. For example
  (a) If the contribution is primarily a new algorithm, the paper should make it clear how to reproduce that algorithm.
  (b) If the contribution is primarily a new model architecture, the paper should describe the architecture clearly and fully.
  (c) If the contribution is a new model (e.g., a large language model), then there should either be a way to access this model for reproducing the results or a way to reproduce the model (e.g., with an open-source dataset or instructions for how to construct the dataset).
  (d) We recognize that reproducibility may be tricky in some cases, in which case authors are welcome to describe the particular way they provide for reproducibility. In the case of closed-source models, it may be that access to the model is limited in some way (e.g., to registered users), but it should be possible for other researchers to have some path to reproducing or verifying the results.

5. **Open access to data and code**

   Question: Does the paper provide open access to the data and code, with sufficient instructions to faithfully reproduce the main experimental results, as described in supplemental material?

   Answer: [No]

   Justification: Our codebase is ready to be released to the public upon acceptance of this submission. However, we do not provide code with the current submission, as our codebase is fairly large and anonymizing it thoroughly poses a risk of inadvertently revealing identifying information.

   Guidelines:

   - The answer NA means that paper does not include experiments requiring code.
   - Please see the NeurIPS code and data submission guidelines (`https://nips.cc/public/guides/CodeSubmissionPolicy`) for more details.
   - While we encourage the release of code and data, we understand that this might not be possible, so "No" is an acceptable answer. Papers cannot be rejected simply for not including code, unless this is central to the contribution (e.g., for a new open-source benchmark).
   - The instructions should contain the exact command and environment needed to run to reproduce the results. See the NeurIPS code and data submission guidelines (`https://nips.cc/public/guides/CodeSubmissionPolicy`) for more details.

- The authors should provide instructions on data access and preparation, including how to access the raw data, preprocessed data, intermediate data, and generated data, etc.
- The authors should provide scripts to reproduce all experimental results for the new proposed method and baselines. If only a subset of experiments are reproducible, they should state which ones are omitted from the script and why.
- At submission time, to preserve anonymity, the authors should release anonymized versions (if applicable).
- Providing as much information as possible in supplemental material (appended to the paper) is recommended, but including URLs to data and code is permitted.

6. **Experimental setting/details**

   Question: Does the paper specify all the training and test details (e.g., data splits, hyper-parameters, how they were chosen, type of optimizer, etc.) necessary to understand the results?

   Answer: [Yes]

   Justification: Table 1 details the datasets and splits. Section 3.2.2 and Section 3.2.3 describe the model architectures and hyperparameter choices, respectively.

   Guidelines:

   - The answer NA means that the paper does not include experiments.
   - The experimental setting should be presented in the core of the paper to a level of detail that is necessary to appreciate the results and make sense of them.
   - The full details can be provided either with the code, in appendix, or as supplemental material.

7. **Experiment statistical significance**

   Question: Does the paper report error bars suitably and correctly defined or other appropriate information about the statistical significance of the experiments?

   Answer: [Yes]

   Justification: We report error bars where applicable. For instance, in Figure 2, each few-shot experiment is repeated three times with different random seeds. The plot displays the mean performance, with the standard deviation shown as shaded regions.

   Guidelines:

   - The answer NA means that the paper does not include experiments.
   - The authors should answer "Yes" if the results are accompanied by error bars, confidence intervals, or statistical significance tests, at least for the experiments that support the main claims of the paper.
   - The factors of variability that the error bars are capturing should be clearly stated (for example, train/test split, initialization, random drawing of some parameter, or overall run with given experimental conditions).
   - The method for calculating the error bars should be explained (closed form formula, call to a library function, bootstrap, etc.)
   - The assumptions made should be given (e.g., Normally distributed errors).
   - It should be clear whether the error bar is the standard deviation or the standard error of the mean.
   - It is OK to report 1-sigma error bars, but one should state it. The authors should preferably report a 2-sigma error bar than state that they have a 96% CI, if the hypothesis of Normality of errors is not verified.
   - For asymmetric distributions, the authors should be careful not to show in tables or figures symmetric error bars that would yield results that are out of range (e.g. negative error rates).
   - If error bars are reported in tables or plots, The authors should explain in the text how they were calculated and reference the corresponding figures or tables in the text.

8. **Experiments compute resources**

Question: For each experiment, does the paper provide sufficient information on the computer resources (type of compute workers, memory, time of execution) needed to reproduce the experiments?

Answer: [Yes]

Justification: We discuss details of compute resources (including type of GPU, memory and average walltime for different kinds of experiments) in Section 3.2.4.

Guidelines:

- The answer NA means that the paper does not include experiments.
- The paper should indicate the type of compute workers CPU or GPU, internal cluster, or cloud provider, including relevant memory and storage.
- The paper should provide the amount of compute required for each of the individual experimental runs as well as estimate the total compute.
- The paper should disclose whether the full research project required more compute than the experiments reported in the paper (e.g., preliminary or failed experiments that didn't make it into the paper).

9. **Code of ethics**

Question: Does the research conducted in the paper conform, in every respect, with the NeurIPS Code of Ethics `https://neurips.cc/public/EthicsGuidelines`?

Answer: [Yes]

Justification: Our work complies with every section of the NeurIPS Code of Ethics. As we do not perform human experiments, the section "Research involving human subjects or participants" does not apply. We use well-known open-source datasets and cite the original sources. Further, our research is foundational and has no direct societal consequences.

Guidelines:

- The answer NA means that the authors have not reviewed the NeurIPS Code of Ethics.
- If the authors answer No, they should explain the special circumstances that require a deviation from the Code of Ethics.
- The authors should make sure to preserve anonymity (e.g., if there is a special consideration due to laws or regulations in their jurisdiction).

10. **Broader impacts**

Question: Does the paper discuss both potential positive societal impacts and negative societal impacts of the work performed?

Answer: [NA]

Justification: Our work is largely a general, foundational analysis into the structure of visual embedding spaces. It intends to enhance the community' understanding of visual representations, and motivate further research questions. As such, we do not see any direct societal impacts. However, we discuss potential impacts in the Conclusion.

Guidelines:

- The answer NA means that there is no societal impact of the work performed.
- If the authors answer NA or No, they should explain why their work has no societal impact or why the paper does not address societal impact.
- Examples of negative societal impacts include potential malicious or unintended uses (e.g., disinformation, generating fake profiles, surveillance), fairness considerations (e.g., deployment of technologies that could make decisions that unfairly impact specific groups), privacy considerations, and security considerations.
- The conference expects that many papers will be foundational research and not tied to particular applications, let alone deployments. However, if there is a direct path to any negative applications, the authors should point it out. For example, it is legitimate to point out that an improvement in the quality of generative models could be used to generate deepfakes for disinformation. On the other hand, it is not needed to point out that a generic algorithm for optimizing neural networks could enable people to train models that generate Deepfakes faster.

- The authors should consider possible harms that could arise when the technology is being used as intended and functioning correctly, harms that could arise when the technology is being used as intended but gives incorrect results, and harms following from (intentional or unintentional) misuse of the technology.
- If there are negative societal impacts, the authors could also discuss possible mitigation strategies (e.g., gated release of models, providing defenses in addition to attacks, mechanisms for monitoring misuse, mechanisms to monitor how a system learns from feedback over time, improving the efficiency and accessibility of ML).

11. **Safeguards**

    Question: Does the paper describe safeguards that have been put in place for responsible release of data or models that have a high risk for misuse (e.g., pretrained language models, image generators, or scraped datasets)?

    Answer: [NA]

    Justification: We only use standard, existing datasets and pre-trained models (*i.e.,* we do not release any new ones). Therefore, our paper does not introduce any risks for misuse.

    Guidelines:

    - The answer NA means that the paper poses no such risks.
    - Released models that have a high risk for misuse or dual-use should be released with necessary safeguards to allow for controlled use of the model, for example by requiring that users adhere to usage guidelines or restrictions to access the model or implementing safety filters.
    - Datasets that have been scraped from the Internet could pose safety risks. The authors should describe how they avoided releasing unsafe images.
    - We recognize that providing effective safeguards is challenging, and many papers do not require this, but we encourage authors to take this into account and make a best faith effort.

12. **Licenses for existing assets**

    Question: Are the creators or original owners of assets (e.g., code, data, models), used in the paper, properly credited and are the license and terms of use explicitly mentioned and properly respected?

    Answer: [Yes]

    Justification: We use widely available datasets that are frequently used in machine learning conferences. We cite the original authors while introducing the datasets in Table 1.

    Guidelines:

    - The answer NA means that the paper does not use existing assets.
    - The authors should cite the original paper that produced the code package or dataset.
    - The authors should state which version of the asset is used and, if possible, include a URL.
    - The name of the license (e.g., CC-BY 4.0) should be included for each asset.
    - For scraped data from a particular source (e.g., website), the copyright and terms of service of that source should be provided.
    - If assets are released, the license, copyright information, and terms of use in the package should be provided. For popular datasets, `paperswithcode.com/datasets` has curated licenses for some datasets. Their licensing guide can help determine the license of a dataset.
    - For existing datasets that are re-packaged, both the original license and the license of the derived asset (if it has changed) should be provided.
    - If this information is not available online, the authors are encouraged to reach out to the asset's creators.

13. **New assets**

    Question: Are new assets introduced in the paper well documented and is the documentation provided alongside the assets?

Answer: [NA]

Justification: We do not release any new assets.

Guidelines:

- The answer NA means that the paper does not release new assets.
- Researchers should communicate the details of the dataset/code/model as part of their submissions via structured templates. This includes details about training, license, limitations, etc.
- The paper should discuss whether and how consent was obtained from people whose asset is used.
- At submission time, remember to anonymize your assets (if applicable). You can either create an anonymized URL or include an anonymized zip file.

14. **Crowdsourcing and research with human subjects**

    Question: For crowdsourcing experiments and research with human subjects, does the paper include the full text of instructions given to participants and screenshots, if applicable, as well as details about compensation (if any)?

    Answer: [NA]

    Justification: Our work does not involve crowdsourcing or researching directly with human subjects.

    Guidelines:

    - The answer NA means that the paper does not involve crowdsourcing nor research with human subjects.
    - Including this information in the supplemental material is fine, but if the main contribution of the paper involves human subjects, then as much detail as possible should be included in the main paper.
    - According to the NeurIPS Code of Ethics, workers involved in data collection, curation, or other labor should be paid at least the minimum wage in the country of the data collector.

15. **Institutional review board (IRB) approvals or equivalent for research with human subjects**

    Question: Does the paper describe potential risks incurred by study participants, whether such risks were disclosed to the subjects, and whether Institutional Review Board (IRB) approvals (or an equivalent approval/review based on the requirements of your country or institution) were obtained?

    Answer: [NA]

    Justification: Our work does not involve crowdsourcing or researching directly with human subjects.

    Guidelines:

    - The answer NA means that the paper does not involve crowdsourcing nor research with human subjects.
    - Depending on the country in which research is conducted, IRB approval (or equivalent) may be required for any human subjects research. If you obtained IRB approval, you should clearly state this in the paper.
    - We recognize that the procedures for this may vary significantly between institutions and locations, and we expect authors to adhere to the NeurIPS Code of Ethics and the guidelines for their institution.
    - For initial submissions, do not include any information that would break anonymity (if applicable), such as the institution conducting the review.

16. **Declaration of LLM usage**

    Question: Does the paper describe the usage of LLMs if it is an important, original, or non-standard component of the core methods in this research? Note that if the LLM is used only for writing, editing, or formatting purposes and does not impact the core methodology, scientific rigorousness, or originality of the research, declaration is not required.

Answer: [Yes]

Justification: We briefly use an LLM to help with generating zero-shot prompts for our experiment in Section 4.4; this has been documented in the same section.

Guidelines:

- The answer NA means that the core method development in this research does not involve LLMs as any important, original, or non-standard components.
- Please refer to our LLM policy (`https://neurips.cc/Conferences/2025/LLM`) for what should or should not be described.

Contents

A Why are vision embeddings rankable?

While theoretical analysis was outside of the scope of our study, we conduct a few further analyses to support our main claims.

A.1 Attribute-wise variability and label noise

We conjecture that rankability along a given ordinal axis is directly related to variability of different attributes in the training data. The wider the attribute distribution, the stronger the optimization pressure may be for rankability to emerge.

Background. In our experiments using CLIP (obtained from timm [72], trained on LAION-400M [58]), we find that rankability for pitch (SRCC = 0.91) is higher compared to rankabilities for yaw (0.31) and roll (0.40). We set out to verify whether the variability of the head orientation angles in LAION-400M face images follows the same trend.

Setup. We randomly sample 100 faces in LAION-400M using a face detection model [43]. We use the same model to estimate yaw, pitch and roll angles of each face. We quantify the variability of each attribute in the LAION-400M dataset using the standard deviations of angles among the 100 faces.

Results and discussion. The standard deviations for pitch, roll and yaw are 21.2, 11.7 and 11.0 degrees, respectively, in LAION-400M. This concurs with the ranking of rankability among the three attributes: pitch $>$ yaw $>$ roll. This corroborates our hypothesis to a certain degree.

As for why CLIP models perform better, we conjecture that label noise present in captions may play a role. Below, we reason via an example.

When training a CLIP model on image-caption pairs that include age-related descriptors, there may often exist ambiguity in the use of age terms. For instance, middle-aged individuals may sometimes be described as "young", while young individuals are described as "middle-aged". However, one rarely describes young individuals as "old". This asymmetric labeling noise may implicitly encourage the model to embed images such that the representations of "young" and "middle-aged" individuals are closer to each other than either of them is to representations of "old" individuals, i.e.,

$$\mathrm{dist}(\text{old}, \text{young}) > \mathrm{dist}(\text{middle-aged}, \text{young}).$$

This may, in turn, indirectly produce the ordinal structure observed in our study.

A.2 Why does DINO outperform CLIP on yaw and roll?

CLIP relies on language supervision. As long as the embedding space places similar image-text pairs together and dissimilar ones apart, there is limited incentive for fine-grained understanding of the image. We hypothesize that LAION-400M also has far fewer captions describing yaw and roll. Intuitively, for yaw, "looking to the left/right" can be ambiguous, and it is even more unnatural to describe roll using language. We verify this intuition empirically by counting the frequency of such phrases in LAION captions: out of approx. 13M captions, pitch is described in approx. 800k captions, yaw in approx. 5k captions while roll is only described in approx. 30 captions. Hence, while there is some incentive to learn pitch, there are reduced incentives for learning yaw and roll.

DINO relies on self-distillation for training, i.e., without language guidance. Additionally, the training process involves several augmentations. As such, fine grained understanding of the visual structure in the image becomes important, likely leading to enhanced coverage of attributes like yaw and roll.

A.3 On which attributes would CLIP significantly outperform DINO?

We observe that CLIP significantly outperforms DINO [47] on image-level attributes like aesthetics and recency. We hypothesize that this can again be explained on the basis of attribute variability. CLIP was pretrained on a largely uncurated dataset (LAION) with very basic caption filters in place. This would have allowed varying qualities of images into CLIP's training pipeline, leading to high variation in quality. On the other hand, DINO's training dataset, LVD-142M, is much better curated, and likely contains only high quality images. Without variation in quality, DINO does not learn much about this attribute.

B Behavior of out-of-scope values

We design an experiment below for analysing *extrapolation* behaviour.

Setup. The UTKFace dataset split used by us (following prior work [78]) contains age labels between 21 and 60. We split the dataset into two subsets: one with ages 21-50 and the other with ages 51-60. We test whether the rank axis obtained over the 21-50 split applies to the 51-60 split by computing the SRCC against the ground-truth labels on the 51-60 split. As a control, we compare against another rank axis computed using the full age range 21-60.

Results and conclusion. We observe that the rank axis obtained on ages 21-50 achieves an SRCC of 0.174 on the 51-60 split, compared to 0.267 when trained on the full range 21-60. Our results suggest that extrapolation is indeed harder than interpolation.

C Results on more attributes

Broadly, our study focuses on four categories of attributes:

- Age progression.
- Geometric understanding (head pose).
- Scene complexity and counting (crowd count).
- Image quality (aesthetics, modernness).

Our reliance on continuously annotated attributes naturally constrains us to this selection. However, a qualitative exploration of other attributes is also interesting; we address this next.

C.1 Ordinal attributes on dSprites

dSprites [38] provides a synthetic testbed for rankability along more "difficult" attributes like color and size.

Setup. We use pretrained CLIP ViT-B/32 embeddings to analyze the rankability of 5 attributes: hue, x-position, y-position, scale, and orientation. For hue, we consider the segment between **red** and **yellow** to avoid cyclicity of the attribute. We compare the no-train, linear, non-linear, and finetuned performances in Table A8.

Table A8: dSprites results.

Attribute	No-train	Linear	Nonlinear	Finetuned
Hue	0.919	0.920	0.996	1.000
PosX	0.551	0.877	0.966	0.998
PosY	0.706	0.966	0.993	0.999
Scale	0.788	0.980	0.985	0.986
Orientation	0.151	0.716	0.908	0.982

Results and discussion. Hue is already well-represented in untrained representations (no-train, 0.919), whereas CLIP pretraining does not seem to boost ordinality (linear, 0.920). We conjecture that hue is often not a discriminatory signal in caption-based contrastive training. Other attributes are significantly better represented (e.g. 0.151 no-train $\rightarrow$ 0.716 linear for orientation). For some attributes, frozen embeddings are as rankable as finetuned ones; for example, scale ordering using rank axis (0.980) vs dedicated fine-tuning (0.986). We conclude that CLIP embeddings are inherently capable of ranking these attributes.

C.2 Qualitative study: "luxuriousness"

We study the rankability of CLIP with respect to "luxuriousness" using images from the "kitchen room & dining room table" class in Open Images V7 [28].

Setup. We randomly sample 20 pairs of images and ask three annotators (in this case, the authors themselves) to answer which image in the pair is more "luxurious". The "ground truth" luxuriousness is determined via majority vote. We measure quality of the rank axis by measuring accuracy of the prediction of the more luxurious image in each pair. The random chance baseline is 0.50 and the upper bound is given by average inter-annotator agreement. We repeat this process over 3 independent trials with different sets of 20 pairs.

Obtaining a rank axis from visual extremes. We prompt GPT-4o [45] to generate two synthetic reference images: one depicting a minimal dining room table setup, while another represents a visually luxurious version of the same scene. We compute the rank axis as the L2-normalized difference between their CLIP image embeddings.

Results. The model achieves an accuracy of 0.75 ± 0.07, well above the random chance accuracy of 0.50 and at the same level as the average inter-annotator agreement of 0.73 ± 0.10. This suggests that CLIP encodes linear ordinal structure to support ranking along semantic attributes like luxuriousness. As shown in the main paper, the rank axis can easily be obtained using just two extreme samples.

D Further details on datasets and dataset-specific results

In the main paper, we present results for each dataset aggregated over all models (Table 2 in the main paper) and rankabilities (Spearman ρ) for each model-dataset pair (Table 3 in the main paper). While the main results convey the primary evidence towards our claim (vision embeddings are rankable), we also report more detailed results on each dataset in this section. Please also refer to Table 1 in the main paper for a condensed overview of all datasets considered.

D.1 Age

UTKFace, introduced in [83], is a dataset of face images with age labels ranging from 0 to 116. Following [78, 27], we use a smaller subset with ages ranging between 21 and 60. The dataset was downloaded from the official website (https://susanqq.github.io/UTKFace/). We report results in Table A9.

Table A9: **UTKFace (Age)**. Spearman's rank correlation ρ across evaluation strategies. **No-train**: linear probe on untrained encoder. **Rankability**: linear probe on pretrained encoder. **Nonlinear**: MLP on frozen encoder. **Finetuned**: encoder + head trained end-to-end. Higher is better.

Model	**No-train** lower bound	**Rankability** main	**Nonlinear** upper bound	**Finetuned** upper bound
ResNet-50	0.212	0.633	0.636	0.762
ViT-B/32	0.283	0.739	0.749	0.737
ConvNeXtV2-L	0.283	0.772	0.776	0.815
DINOv2 ViT-B/14	0.054	0.770	0.770	0.812
OpenAI CLIP ResNet-50	0.130	0.820	0.830	0.790
OpenAI CLIP ViT-B/32	0.250	0.810	0.830	0.830
OpenCLIP ConvNeXt-L (D, 320px)	0.180	0.820	0.840	0.850
Mean	0.199	0.766	0.776	0.799

Adience, introduced in [11], is another age dataset. Unlike UTKFace, it contains coarse labels (8 age groups instead of exact ages). We use the “aligned” version of the images and five-fold cross-validation as in [78]. Results can be found in Table A10.

Table A10: **Adience (Age)**. Spearman's rank correlation ρ across evaluation strategies.

Model	**No-train** lower bound	**Rankability** main	**Nonlinear** upper bound	**Finetuned** upper bound
ResNet-50	0.328	0.723	0.759	0.894
ViT-B/32	0.310	0.828	0.860	0.892
ConvNeXtV2-L	0.522	0.871	0.885	0.910
DINOv2 ViT-B/14	0.120	0.853	0.877	0.914
OpenAI CLIP ResNet-50	0.070	0.898	0.914	0.894
OpenAI CLIP ViT-B/32	0.292	0.924	0.922	0.928
OpenCLIP ConvNeXt-L (D, 320px)	0.220	0.928	0.932	0.938
Mean	0.266	0.861	0.878	0.910

D.2 Crowd count

UCF-QNRF, introduced in [7], is a large crowd counting dataset containing images from diverse parts of the world. We use the official download link at https://www.crcv.ucf.edu/data/ucf-qnrf/ and the official train-test splits. Results can be found in Table A11.

Table A11: **UCF-QNRF (Crowd Count)**. Spearman's rank correlation ρ across evaluation strategies.

Model	**No-train** lower bound	**Rankability** main	**Nonlinear** upper bound	**Finetuned** upper bound
ResNet-50	0.466	0.864	0.870	0.826
ViT-B/32	0.288	0.837	0.840	0.794
ConvNeXtV2-L	-0.054	0.810	0.816	0.938
DINOv2 ViT-B/14	0.219	0.788	0.842	0.961
OpenAI CLIP ResNet-50	0.240	0.870	0.880	0.820
OpenAI CLIP ViT-B/32	0.280	0.870	0.870	0.900
OpenCLIP ConvNeXt-L (D, 320px)	0.100	0.860	0.860	0.960
Mean	0.220	0.843	0.854	0.886

ShanghaiTech, introduced in [82], is another crowd counting dataset consisting of two parts: A and B. While part A was crawled from the Internet and features larger crowds in general, part B was taken from metropolitan areas of Shanghai and features much smaller crowds. We use the DropBox link available at https://github.com/desenzhou/ShanghaiTechDataset and official train-test splits for both parts. Results can be found in Table A12 and Table A13.

Table A12: **ShanghaiTech-A (Crowd Count)**. Spearman's rank correlation ρ across evaluation strategies.

Model	**No-train** lower bound	**Rankability** main	**Nonlinear** upper bound	**Finetuned** upper bound
ResNet-50	0.359	0.799	0.802	0.529
ViT-B/32	0.148	0.700	0.623	0.558
ConvNeXtV2-L	0.061	0.695	0.753	0.834
DINOv2 ViT-B/14	-0.017	0.653	0.722	0.786
OpenAI CLIP ResNet-50	0.200	0.760	0.770	0.510
OpenAI CLIP ViT-B/32	0.010	0.750	0.770	0.700
OpenCLIP ConvNeXt-L (D, 320px)	0.080	0.780	0.800	0.910
Mean	0.120	0.734	0.749	0.689

Table A13: **ShanghaiTech-B (Crowd Count)**. Spearman's rank correlation ρ across evaluation strategies.

Model	**No-train** lower bound	**Rankability** main	**Nonlinear** upper bound	**Finetuned** upper bound
ResNet-50	0.280	0.879	0.906	0.672
ViT-B/32	0.225	0.878	0.889	0.710
ConvNeXtV2-L	0.070	0.867	0.876	0.955
DINOv2 ViT-B/14	0.020	0.821	0.869	0.972
OpenAI CLIP ResNet-50	0.270	0.890	0.900	0.690
OpenAI CLIP ViT-B/32	0.040	0.860	0.860	0.900
OpenCLIP ConvNeXt-L (D, 320px)	0.040	0.890	0.910	0.980
Mean	0.135	0.869	0.887	0.840

D.3 Headpose (Euler angles)

The **BIWI Kinect** dataset, introduced in [13], is a collection of 24 different videos wherein the subject of the video sits about a meter away from a Kinect (https://en.wikipedia.org/wiki/Kinect) sensor and rotates their head to span the entire range of possible head-pose angles pitch (rotation about the x-axis), yaw (rotation about the y-axis) and roll (rotation about the z-axis). As there exists no official split that we know of, we randomly hold out 6 sequences for testing. Results can be found in Table A14 (pitch), Table A15 (yaw) and Table A16 (roll).

Table A14: **Kinect (Pitch)**. Spearman's rank correlation ρ across evaluation strategies.

Model	**No-train** lower bound	**Rankability** main	**Nonlinear** upper bound	**Finetuned** upper bound
ResNet-50	0.359	0.663	0.615	0.973
ViT-B/32	0.401	0.673	0.505	0.951
ConvNeXtV2-L	0.548	0.909	0.882	0.984
DINOv2 ViT-B/14	0.231	0.716	0.986	0.979
OpenAI CLIP ResNet-50	0.450	0.860	0.870	0.970
OpenAI CLIP ViT-B/32	0.400	0.920	0.940	0.980
OpenCLIP ConvNeXt-L (D, 320px)	0.450	0.880	0.880	0.990
Mean	0.405	0.803	0.811	0.975

Table A15: **Kinect (Yaw)**. Spearman's rank correlation ρ across evaluation strategies.

Model	**No-train** lower bound	**Rankability** main	**Nonlinear** upper bound	**Finetuned** upper bound
ResNet-50	0.160	0.624	0.726	0.990
ViT-B/32	0.209	0.305	0.305	0.838
ConvNeXtV2-L	0.113	0.384	0.716	0.989
DINOv2 ViT-B/14	−0.046	0.804	0.871	0.994
OpenAI CLIP ResNet-50	−0.060	0.120	0.530	0.980
OpenAI CLIP ViT-B/32	0.160	0.360	0.330	0.990
OpenCLIP ConvNeXt-L (D, 320px)	0.010	0.440	0.700	0.990
Mean	0.078	0.434	0.597	0.967

Table A16: **Kinect (Roll)**. Spearman's rank correlation ρ across evaluation strategies.

Model	**No-train** lower bound	**Rankability** main	**Nonlinear** upper bound	**Finetuned** upper bound
ResNet-50	0.202	0.352	0.430	0.930
ViT-B/32	0.098	0.196	0.375	0.477
ConvNeXtV2-L	0.550	0.298	0.368	0.963
DINOv2 ViT-B/14	0.256	0.512	0.551	0.912
OpenAI CLIP ResNet-50	0.140	0.090	0.300	0.920
OpenAI CLIP ViT-B/32	−0.060	0.020	0.170	0.850
OpenCLIP ConvNeXt-L (D, 320px)	−0.130	0.060	0.090	0.960
Mean	0.151	0.218	0.326	0.859

D.4 Aesthetics (Mean Opinion Score)

The **Aesthetics Visual Analysis (AVA)** dataset, introduced in [41], is a large-scale dataset including aesthetic preference scores provided by human annotators. Each image is labeled by multiple annotators, each assigning a score in the range 1-10. The mean opinion score (MOS) of the image is then computed as a weighted average over the ratings where the weight of a rating is provided by its frequency. We use the split provided by [78] in their official repository (https://github.com/uynaes/RankingAwareCLIP/tree/main/examples). Results are reported in Table A17.

Table A17: **AVA (Image Aesthetics)**. Spearman's rank correlation ρ across evaluation strategies.

Model	**No-train** lower bound	**Rankability** main	**Nonlinear** upper bound	**Finetuned** upper bound
ResNet-50	0.237	0.589	0.628	0.672
ViT-B/32	0.157	0.609	0.666	0.672
ConvNeXtV2-L	0.158	0.644	0.685	0.728
DINOv2 ViT-B/14	0.057	0.566	0.648	0.590
OpenAI CLIP ResNet-50	0.150	0.700	0.710	0.700
OpenAI CLIP ViT-B/32	0.200	0.710	0.730	0.700
OpenCLIP ConvNeXt-L (D, 320px)	0.130	0.750	0.780	0.790
Mean	0.156	0.653	0.692	0.693

KonIQ-10k, introduced in [17], is another aesthetics or image quality assessment (IQA) dataset that aims to model naturally occurring image distortions with mean opinion scores ranging roughly between 1 and 100. We use the official train-test splits. Results can be found in Table A18.

Table A18: **KonIQ-10k (Image Aesthetics)**. Spearman's rank correlation ρ across evaluation strategies.

Model	**No-train** lower bound	**Rankability** main	**Nonlinear** upper bound	**Finetuned** upper bound
ResNet-50	0.563	0.739	0.739	0.874
ViT-B/32	0.488	0.713	0.753	0.813
ConvNeXtV2-L	0.487	0.744	0.765	0.930
DINOv2 ViT-B/14	0.324	0.681	0.753	0.948
OpenAI CLIP ResNet-50	0.400	0.800	0.840	0.900
OpenAI CLIP ViT-B/32	0.460	0.790	0.830	0.890
OpenCLIP ConvNeXt-L (D, 320px)	0.320	0.860	0.870	0.950
Mean	0.435	0.761	0.793	0.901

D.5 Image recency

Historical Color Images (HCI), introduced in [49], was designed for the task of classifying an image by the decade during which it was taken. Therein emerges a natural ordering over the decades, defining the ordinal attribute of image "modernness" or "recency". We use the split provided by [78] in their repository (https://github.com/uynaes/RankingAwareCLIP/tree/main/examples) and report the results in Table A19.

Table A19: **HCI (Historical Color Images)**. Spearman's rank correlation ρ across evaluation strategies.

Model	**No-train** lower bound	**Rankability** main	**Nonlinear** upper bound	**Finetuned** upper bound
ResNet-50	0.351	0.600	0.592	0.614
ViT-B/32	0.377	0.592	0.618	0.529
ConvNeXtV2-L	0.362	0.631	0.663	0.771
DINOv2 ViT-B/14	0.131	0.571	0.601	0.748
OpenAI CLIP ResNet-50	0.320	0.780	0.770	0.760
OpenAI CLIP ViT-B/32	0.430	0.770	0.780	0.760
OpenCLIP ConvNeXt-L (D, 320px)	0.300	0.820	0.790	0.870
Mean	0.324	0.680	0.688	0.722

E Comparison with existing works

Our main aim in this work is to understand the rankability emerging out of the structure in visual embedding spaces, and we contextualize our numbers using reference metrics (lower bound provided by the no-encoder baseline and upper bound provided by nonlinear regression and finetuned encoders). This section additionally provides comparisons with prior work to further support our claims.

E.1 Comparison with SOTA works

Prior research has presented results from dedicated or general efforts to solve the datasets considered in our study. Such works often require modification of the entire encoder or final embeddings, with dedicated loss functions or even architectural changes. This significantly limits adaptability. For each new attribute to rank a dataset, a user needs to employ a considerable amount of compute to train a dedicated embedding.

In Table A20, we also provide comparisons with such state-of-the-art results to further contextualize our results. Although architectural and training dataset differences mean that this comparison is not always fair, we emphasize the contrast in implementational simplicity between dedicated efforts and simple linear regression over pretrained embeddings that are often readily available and easy to use. Our comparisons suggest that many existing off-the-shelf encoders contain sufficient information to rank datasets according to common attributes and simple linear regression over pretrained embeddings is a strong baseline that must be considered before developing dedicated regression methods (please see next page for Table A20).

Table A20: **Comparing linear / nonlinear regression against recent state-of-the-art methods.** “Linear” and “Nonlinear” use regression over CLIP-ConvNeXt-L embeddings. Dashes indicate metrics unreported in prior work. We take the numbers for age, aesthetics and recency from [78], and crowd count from [37]. Under “Downstream model”, we report the components used on top of pretrained visual embeddings (CLIP or non-CLIP models); sometimes, we also report if the encoder itself was retrained. Under “Downstream data”, we report the additional data used for training the method. Finally, under “Other ingredients”, we also report miscellaneous extra components used by the corresponding method. All method interpretations are to the best of our knowledge.

Attribute	**Dataset**	**Method**	**Spearman ρ**	**MAE**	**Downstream model**	**Downstream data**	**Other ingredients**
Age	UTKFace	Yu et al. [78]	–	3.83	Cross-attn encoder, two ranking heads, learnable text prompt tokens	Images with age labels	Text encoder
		MiVOLO [27]	–	4.23	Regression heads	Body images, face patches, age labels	Feature enhancer module for fused joint representations
		Linear	–	4.25	Linear regressor	Images with age labels	None
		Nonlinear	–	4.10	2-layer MLP regressor	Images with age labels	None
Age	Adience	Yu et al. [78]	–	0.36 (0.03)	Cross-attn encoder, two ranking heads, learnable text prompt tokens	Images with age labels	Text encoder
		OrdinalCLIP [34]	–	0.47 (0.06)	(Retrain image encoder for the task)	Images with age labels	Text encoder; learn “continuous” rank prototype (text) embeddings for each rank
		Linear regressor	–	0.48 (0.02)	Linear	Images with age labels	None
		Nonlinear	–	0.45 (0.02)	2-layer MLP regressor	Images with age labels	None
Crowd Count	UCF-QNRF	CLIP-EBC [37]	–	80.3	Blockwise classification module	Images with count labels	Text encoder
		CrowdCLIP [35]	–	283.3	(Retrain image encoder)	Crowd images	Text encoder, three-stage progressive filtering during inference
		Linear	–	246.4	Linear	Images with count labels	None
		Nonlinear	–	248.0	2-layer MLP	Images with count labels	None
Crowd Count	ST-A	CLIP-EBC [37]	–	52.5	Blockwise classification module	Images with count labels	Text encoder
		CrowdCLIP [35]	–	146.1	(Retrain image encoder)	Crowd images	Text encoder, three-stage progressive filtering during inference
		Linear	–	167.1	Linear	Images with count labels	None
		Nonlinear	–	151.7	2-layer MLP	Images with count labels	None
Crowd Count	ST-B	CLIP-EBC [37]	–	6.6	Blockwise classification module	Images with count labels	Text encoder
		CrowdCLIP [35]	–	69.3	(Retrain image encoder)	Crowd images	Text encoder, three-stage progressive filtering during inference

Continued on next page

Table A20 – *Continued from previous page*

Attribute	Dataset	Method	Spearman ρ	MAE	Downstream model	Downstream data	Other ingredients
		Linear	–	34.7	Linear	Images with count labels	None
		Nonlinear	–	29.7	2-layer MLP	Images with count labels	None
Aesthetics	AVA	Yu et al. [78]	0.747	–	Cross-attn encoder, two ranking heads, learnable text prompt tokens	Images with MOS labels (1–10)	Text encoder
		CLIP-IQA [67]	0.415	–	Softmax over two similarity scores	None	Text encoder, prompt engineering, remove position embedding
		Linear	0.749	–	Linear	Images with MOS labels(1–10)	None
		Nonlinear	0.775	–	2-layer MLP	Images with MOS labels (1–10)	None
Aesthetics	KonIQ-10k	Yu et al. [78]	0.911	–	Cross-attn encoder, two ranking heads, learnable text prompt tokens	Images with MOS labels (1–100)	Text encoder
		CLIP-IQA [67]	0.727	–	Softmax over two similarity scores	None	Text encoder, prompt engineering, remove position embedding
		Linear	0.860	–	Linear	Images with MOS labelss (1–100)	None
		Nonlinear	0.870	–	2-layer MLP	Images with MOS labels (1–100)	None
Recency	HCI	Yu et al. [78]	–	0.32 (0.03)	Cross-attn encoder, two ranking heads, learnable text prompt tokens	Images with decade labels	Text encoder
		OrdinalCLIP [34]	–	0.67 (0.03)	(Retrain image encoder for the task)	Images with decade labels	Text encoder; learn “continuous” rank prototype (text) embeddings for each rank
		Linear	–	0.64	Linear	Images with decade labels	None
		Nonlinear	–	0.60	2-layer MLP	Images with decade labels	None

E.2 Is the finetuning upper bound good enough?

While we train our finetuned (upper bound) models using regular MSE loss, there exist specialised ranking loss functions introduced in prior works that we will refer to as GOL [29] and RnC [81]. While direct comparisons training the encoders used in our main paper using the loss functions from GOL and RnC were infeasible because of resource constraints, we confirm using a small ablation whether finetuning is a strong-enough upper bound for our analysis. We achieve this by comparing finetuning with MSE loss against the loss functions proposed in [29, 81].

Table A21: Comparison with GOL [29]

Linear	Nonlinear	Finetuned	GOL
7.06	6.23	4.88	4.35

Table A22: Comparison with RnC [81].

Linear [ResNet18; DINO]	Nonlinear [ResNet18; DINO]	FT [ResNet18]	RnC
9.97; 8.18	9.50; 7.76	6.57	6.14

Observations and conclusions.

We present our findings in Table A21 and Table A22. We observe that standard finetuning using MSE loss on downstream tasks (using the same or similar models) yields performance quite close to that of [29, 81]. On UTKFace and AgeDB [40], finetuned VGG16 and ResNet18 models achieve MAEs of 4.88 and 6.57, only modestly outperformed by [29] (4.35) and RnC [81] (6.14), respectively. For RnC, we use the ResNet18 model from `timm` while theirs was trained from scratch, however, for GOL, we used the same initial weights as [29].

We emphasize that our goal is complementary to GOL and RnC: while they propose methods for improving rank estimation, our study aims to evaluate rankability already present in off-the-shelf visual embeddings. Given our primary focus on probing intrinsic structure of pretrained embeddings using architecture-agnostic tools, and that finetuning itself already reduces the gap significantly, we conclude that finetuning provides a sufficiently strong upper bound for our analysis.